Short-term performance impairment in adaptive reaching following exercise induced neuromuscular fatigue in lower-limb postural muscles

Mauro Nardon[1], Oindrila Sinha[2], John Kpankpa[2], Eliza Albenze[2], Cédrick Bonnet[3], Matteo Bertucco[1#], Tarkeshwar Singh[2#*]

[1]Department of Neurosciences, Biomedicine and Movement Sciences, University of Verona, Via Casorati, 43, Verona, 37131, Italy
[2]Department of Kinesiology, The Pennsylvania State University, University Park, PA-16802, USA
[3]Univ. Lille, CNRS, UMR 9193-SCALab-Sciences Cognitives et Sciences Affectives, Lille, France

# These authors share senior authorship.
* Corresponding author.

Running Head (max 60 chr):
Postural muscles fatigue affects force field adaptation

Keywords: Motor adaptation; muscle fatigue; posture; postural control, reaching.

* Corresponding author:
Dr. Tarkeshwar Singh
Department of Kinesiology, The Pennsylvania State University, University Park, PA-16802, USA
Email: tsingh@psu.edu

Abstract

Neuromuscular fatigue (NMF) induces temporary reductions in muscle force production capacity, affecting various aspects of motor function. While studies have extensively explored NMF's impact on muscle activation patterns and postural stability, its influence on motor adaptation processes remains less understood. This paper investigates the effects of localized NMF on motor adaptation during upright stance, focusing on reaching tasks. Utilizing a force field perturbation paradigm, participants performed reaching movements while standing upright before and after inducing NMF in the ankle dorsiflexor muscles. Results revealed that despite maintained postural stability, participants in the NMF group exhibited larger movement errors during reaching tasks, suggesting impaired motor adaptation. This was evident in both initial and terminal phases of adaptation, indicating a disruption in learning processes rather than a decreased adaptation rate. Analysis of electromyography (EMG) activation patterns highlighted distinct strategies between groups, with the NMF group showing altered activation of both fatigued and non-fatigued muscles. Additionally, differences in co-activation patterns suggested compensatory mechanisms to maintain postural stability despite NMF-induced disruptions. These findings underscore the complex interplay between NMF, motor adaptation, and postural control, suggesting a potential role for central nervous system mechanisms in mediating adaptation processes. Understanding these mechanisms has implications for sports performance, rehabilitation, and motor skill acquisition, where NMF may impact the learning and retention of motor tasks. Further research is warranted to elucidate the transient or long-term effects of NMF on motor adaptation and its implications for motor rehabilitation interventions.

New & Noteworthy

We assessed motor adaptation during force field reaching following exercise-induced neuromuscular fatigue (NMF) on postural muscles. NMF impaired adaptation in performance. Similarly, diverging activation strategies were observed in the muscles. No effects were seen on measures of postural control. These results suggest the remodulation of motor commands to the muscles in presence of NMF, which may be relevant in settings where participants could be exposed to NMF while learning, such as sports and rehabilitation.

Introduction

Exercise-induced neuromuscular fatigue (NMF) is characterized by a temporary reduction in the ability of a muscle to produce force and/or power, (1–3). This phenomenon affects various dimensions of human motor function, including the planning of motor activities (4–7), coordination (8–11), balance (12), sensorimotor integration (13, 14), limb proprioception (15, 16) and muscle activation patterns (17). Furthermore, NMF adversely affects gait characteristics (18–21) and posture stabilization (22–24). Specifically, NMF leads to postural instability by enhancing the sway velocity of the center of pressure (22) and diminishing the efficacy of balance recovery following disturbances (25). Contrarily, some investigations have reported no direct impact of NMF on postural stability metrics, despite noting variations in muscle activation patterns (17, 26). These alterations in muscle activation post-NMF are interpreted by subsequent analyses as efficient adaptations by the central nervous system (CNS) to counteract NMF and preserve postural steadiness (4, 17, 23, 24, 26).

Exercise-induced unilateral NMF induces central adaptations that manifest as adaptive (and sometimes maladaptive) adjustments in the motor output of the contralateral, non-exercised limb (27, 28). This phenomenon, known as non-local muscle fatigue, involves performance alterations in contralateral or distant, non-exercised muscle groups. It is primarily mediated by central mechanisms and is believed to involve neural structures responsible for coordinating bilateral and unilateral movements between the upper and lower extremities (29). Notably, the cerebellum, which plays a crucial role in the integration of proprioceptive inputs for the real-time and offline control of movements, may also support fatigue induced central adaptations in the descending drive to exercised and unexercised muscles. Indeed, recent evidence indicates that a reduction in cerebellar excitability is associated with an altered perception of fatigue and changes during visuomotor adaptation (30). Considering the cerebellum's role in coordinating bilateral movements (31, 32), and integrating motor functions between the upper and lower body (33) it is conceivable that NMF significantly impacts motor functions through cerebellar mediation, such as during motor adaptation tasks.

The motor adaptation paradigm, which investigates the sensorimotor system's ability to recalibrate in response to experimental perturbations, has been instrumental in establishing the cerebellum as a critical component of the neural circuitry facilitating adaptation (34–38). Within this paradigm, the force field adaptation approach involves participants executing reaching movements under conditions of artificially induced perturbations, such as velocity-dependent viscous or curl force fields generated by robots, thereby learning to recalibrate their motor output in response to altered proprioceptive feedback on a trial-by-trial basis (39).

A study by Takahashi and colleagues (40) revealed that NMF can impair the development and retention of a recalibrated mapping between altered proprioceptive feedback and motor output necessary to perform a force field reaching task. This finding implies that NMF may specifically influence adaptation in unilateral upper-extremity tasks, but it also raises questions about whether such interference is localized to the limb engaged in the exercise or if adaptive (or maladaptive) modifications extend to non-exercised limbs, thereby affecting overall performance and coordination. Addressing this question would enhance our comprehension of the mechanisms by which the nervous system concurrently maintains global postural stability and facilitates movement through localized activation of upper limb musculature.

A simple approach to explore this question would involve conducting a force field reaching task during upright stance. Ahmed and Wolpert (41) utilized this paradigm and compared the transferability of learned novel force field dynamics between seated and upright standing conditions. Their findings demonstrated that participants not only learned the novel dynamics but also successfully generalized these learnings across different postural stances (from seated to standing and vice versa). Additionally, from the onset of trials, individuals exhibited the capability for making pertinent anticipatory postural adjustments while standing. Collectively, these results imply that the networks responsible for posture stabilization and movement coordination can concurrently manage different motor functions to adeptly navigate actions within new dynamic environments.

Based on these disparate sets of studies, we hypothesized that the nervous system maintains postural stability and movement accuracy during NMF by modulating the central descending drive to muscles. Based on this hypothesis, we predict alterations in the activation patterns of both exercised and unexercised muscles to maintain reaching accuracy and stabilize center-of-pressure dynamics during a force field adaptation task. We tested this prediction using an experimental task where participants performed reaching movements under a force field while standing upright.

Materials and Methods

Participants

Twenty-eight right-handed, healthy young participants (14 males; 14 females) were randomly assigned to either a *Fatigue* or *No-Fatigue* group. Participants were excluded if they had a history of neurological or musculoskeletal disorders, cardiovascular disease that would make it difficult to perform the exercises, and conditions of the vestibular system that would affect balance. Participants were also excluded if they took medications which made them drowsy and would affect upright posture control. The study protocol conformed to the most recent principles of the Declaration of Helsinki and was approved by the Institutional Review Board (IRB) of

The Pennsylvania State University. Participants provided written informed consent before taking part in the study. Participants' demographics are reported in ***Table 1***.

Table 1. Participants demographics divided into groups.

Group (F/M)	**Age (years)**	**Weight (kg)**	**Height (cm)**
Fatigue (7/7)	22.4 ± 2.9	69.3 ± 13.4	171.9 ± 10
No-Fatigue (7/7)	22.3 ± 4	67.2 ± 12.9	169.6 ± 7.9

Values are reported as mean ± SD. F: Females, M: Males.

Apparatus

Experiments were carried out employing a unimanual *KINARM* End-Point robot (Kinarm Inc, Kingston, Canada), in an adjustable height configuration for conducting reaching studies during upright stance. The system was integrated with a force plate (FP4060-07-TM, Bertec, Columbus, OH, USA) positioned in front of the center of the robot screen. Participants' safety was ensured by using a full-body harness, connected by carabiners to an overhead metal rack (max operating weight and height range: 163 kg and 97-213 cm, respectively; **Figure 1** A).

Electromyographic (EMG) activity of eleven muscles – three in the upper right limb (*anterior deltoid* (AD), *posterior deltoid* (PD), and *triceps brachii* (TR) and four each in both the lower limbs, bilaterally (*rectus femoris* (RF), *biceps femoris* – long head (BF), *tibialis anterior* (TA), *gastrocnemius medialis* (GM) – was recorded using wireless EMG sensors (Trigno, Delsys Inc., Natick, MA, USA). Sensor positioning was conducted following recommendations (42), signal baseline noise and signal-to-noise ratio were inspected using the dedicated software (*EMGWorks*, Delsys Inc.) to ensure high EMG signal quality. EMG signals were digitized and synchronized with robot kinetics and kinematics, and with force-plate data through an A/D converter (National Instruments) and automatically streamed to the computer running the robot data-acquisition software (Dexterit-E™, Kinarm Inc, Kingston, ON, Canada). Data from the robotic manipulandum, force plate and EMG were synchronized and sampled at 1000 Hz.

A customized frame equipped with a uniaxial strain-gauge force sensor (Model S-AL-A, Deltatech, Sogliano al Rubicone, Italy) was used for the force measurement during the isometric fatiguing task (see *Procedures*) to measure isometric force in ankle dorsiflexion. Force data were collected using a custom LabVIEW VI (National Instruments) software at 50 Hz sampling rate. Signals were exported and analyzed offline using MATLAB (R2023a, version 9.14.0, MathWorks, Natick, MA, USA).

Procedures

Participants were given an overview of the experiment and received specific instructions: 1) avoid leaning the forehead on the Kinarm while standing; and 2)

avoid pulling the robot handle downward. They first performed 10 (unperturbed) trials to familiarize with the reaching task. Few additional isometric trials (*normTrials*) were performed to be used for EMG normalization.

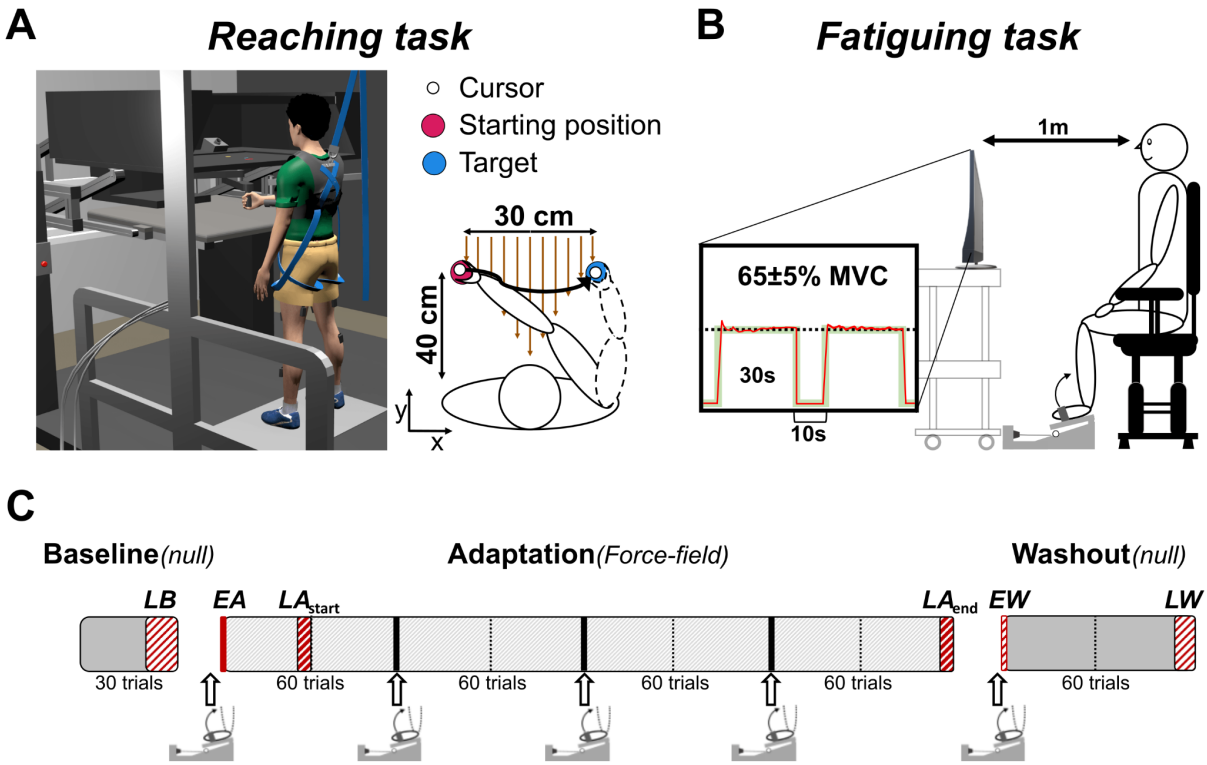

Figure 1

Schematic representation of the experimental setup. A: experimental setup (Side view) of the reaching task on the KINARM robot screen (Top view). Brown, vertical arrows represent the direction of force field perturbation, while the black solid line represents the cursor trajectory during a reaching movement. Laboratory axes orientation is shown at the bottom-left corner. B: illustration for the isometric ankle dorsiflexion exercise setup for the fatiguing of tibialis anterior muscles. Knee and ankle joint angles were kept ~90° and 110° throughout the exercise. Real-time visual feedback of the force was provided by a monitor, which also displayed a green-shaded area corresponding to the required force target (Fatigue= 65 ± 5%, No-Fatigue= 7.5 ± 5% MVC). C: schematic outline of the experimental phases: baseline phase consisted of 30 unperturbed (null) reaching trials, learning phase consisted of 240 perturbed (force field) trials divided into 4 blocks of 60 trials and washout phase consisted of 60 null trials. Bottom isometric setup-like symbols indicate the fatiguing exercise bouts (see Isometric Task in the text). Thin vertical dotted lines separating learning and washout blocks represent short breaks (<1min) in between two blocks of 30 trials during the learning and washout phases (see Reaching Task in the text). Experimental phases considered for the analyses are highlighted in red. LB: late baseline, EA: early adaptation, LA_{start}: late adaptation – start, LA_{end}: late adaptation – final block, EW: early washout, LW: late washout.

Reaching Task

Participants stood barefoot on the force plate, in front of the robot screen. Feet positions were checked and marked on the force platform to ensure consistency

across experimental blocks. KINARM screen and handle height was adjusted to each participant's height to ensure comfortable range of movement. The task consisted of planar reaching movements in the medio-lateral direction (range: 30 cm). Participants' vision of the hand was occluded by the screen during the trials and they were required to move the cursor (radius: 1 cm) – corresponding to the hand position – to the location of the targets on the screen. Targets were within reach of the participant and did not require trunk movement. The starting position (start) consisted of a circle (radius: 1.5 cm; positioned 5 cm left from the mid-sagittal plane, ~40 cm away from participant's chest). Once reached, the data acquisition started and participants were instructed to maintain the cursor in this location until a second target (radius: 1.5 cm) appeared 30 cm to the right (**Figure 1** A) and reach for it as quickly and accurately as possible. Targets color changed when reached by the participant. The experiment was programmed to display the target with a fixed (1,500 ms) plus a random delay (1-500 ms) after *start* had been reached to avoid predictability of the stimulus and its anticipation. If participants moved the cursor before the target appeared, the trial was aborted and repeated. Participants were instructed to return to *start* at a comfortable pace. Immediately after familiarization, participants performed a block (*baseline*; 30 trials) of unperturbed (*null*) reaching movements. During the subsequent experimental phase (*learning;* 240 trials), the robot simulated a viscous curl field (*force field*) by generating a force (*F*) perpendicular (clockwise) to the direction and proportional to the magnitude of the instantaneous velocity (*V*) of the robot handle:

$$\begin{bmatrix} F_X \\ F_Y \end{bmatrix} = k \begin{bmatrix} 0 & -1 \\ 1 & 0 \end{bmatrix} \begin{bmatrix} V_X \\ V_Y \end{bmatrix}$$

Where the field gain *k* was set to 0.2 N*s/cm. The last experimental phase (*washout*; 60 trials) consisted of unperturbed (*null*) trials. In order to avoid fatigue in the upper limb, participants were allowed short breaks (<1min) to relax their arm and posture halfway (every 30 trials) in *learning* and *washout* blocks. This was based on pilot work conducted in the laboratory prior to the study. Handle position, velocity and the force applied at the handle, ground reaction forces (GRFs), center of pressure (CoP) and surface EMG data were recorded during each trial.

Isometric Fatiguing Task

Participants seated on a height-adjustable chair with their feet fastened to a customized metal frame through two inextensible straps, placed proximal to the metatarsophalangeal joints (**Figure 1** B). Knee and ankle joint angles were maintained at approximately 90° and 110°, respectively and the position did not change throughout the entire experimental session. To avoid the involvement of other postural and upper limb muscles, participants were instructed to place and keep their hands prone on their thighs.

Participants performed three ~5 s maximal voluntary contractions (MVCs) in isometric dorsiflexion of the ankles, using mainly both their tibialis anterior (TA) muscles. MVCs were inspected and the highest value was used to set the relative exercise intensity. To ensure maximal effort and avoid errors in the MVC determination, if one of the MVCs value differed more than 10% from the others, the value was discarded and an additional MVC trial was performed. Participants rested for >1 min between consecutive MVCs.

Sustained, cyclical isometric exercise protocol (40 seconds; 75% duty cycle) was set relative to each participant's MVC value and differed between groups (Fatigue: 65 ± 5%; No-Fatigue: 7.5 ± 5% MVC) (43). This ensured that both groups went through identical experimental protocols, but only one group was fatigued. This resulted with induced localized neuromuscular muscle fatigue on the main ankle dorsiflexor muscles – TAs for the Fatigue group. A computer monitor (22"; viewable diagonal screen size 54.8 cm), placed ~1 m away at participant's eye level, provided real-time visual feedback on the force production during the exercise while an audible timer set the pace of the exercise-rest phases of the protocol. Participants were asked to keep the force – shown as a black dot – within the target force boundaries, displayed on the monitor screen as a green-shaded area throughout the entire exercise phase (30s) of the cycle and successively relax for the remaining 10s of the cycle. Participants in the Fatigue group were considered fatigued and stopped when their force did not reach and sustain for >1s the target force for two consecutive cycles despite continuous encouragement. Few seconds later, participants were asked to produce an additional MVC and then asked to move back to the reaching task and immediately perform the subsequent movement block (≤30 s).

Mean exercise time for each bout (each exercise in between blocks of reaching task) of isometric tasks of the Fatigue group was calculated and rounded up to the nearest cycle (40s). These exercise times were later used to stop participants in the No-Fatigue group (exercising around 7.5% MVC). This was done to ensure a similar time duration in both groups and required the entire Fatigue group to be tested before No-Fatigue. Participants in both groups were stopped by the experimenter and were blind to exercise intensity (%MVC), termination criteria and exercise bouts duration. The isometric exercise setup was positioned ~1.5 meters away from the robot to ensure a rapid transition between the tasks.

Since NMF is a transient phenomenon (10, 44, 45), fatiguing exercise was repeated multiple times throughout the experiment to limit recovery processes. To assess the effects of NMF on motor adaptation, we computed performance variables, postural stability measures and EMG activity during anticipatory (AP) and corrective windows – here we define EMG activity occurring after movement initiation as early- and voluntary Reactive Responses (eRR and vRR, respectively).

Data Analysis

Computed variables were compared at six phases of the experiment: *late baseline* (LB; last 10 trials in baseline phase); *early adaptation* (EA; 1st trial in learning phase); *late adaptation – start* (LA_{start}; 27th–30th trial); *late adaptation – final* (LA_{end}; last 5 trials in *learning* phase); *early washout* (EW; 1st trial in *washout* phase); *late washout* (LW; last 5 trials in *washout* phase). Separate planned comparisons were performed across phases: 1) LB, EA, LA1, LA_{end}; and 2) LB, EW, LW, to assess adaptation rate and *washout* phase effects, respectively, in accordance with previous similar studies (41, 46, 47). A schematic outline of the experiment and the relative phases is shown in **Figure 1** (C).

Handle kinematics and force plate signals were filtered with a 10 Hz low-pass, 6th order, zero-phase digital Butterworth filter. EMG signals were detrended, band-pass filtered with a 20–450 Hz, 4th order, zero-phase digital Butterworth filter and rectified, then a 57–63 Hz, band-stop, 4th order filter was applied to remove line noise. Hand movement onset (*t0*) was calculated as the point in time when hand force profile in the mediolateral direction crossed 5% of its peak value (similar to (48) - **Figure 2**). EMG, hand kinematics and force plate signals were then aligned from 500 ms before- to 1,000 ms after *t0* and stored for further analyses. EMG signals from *normTrials* were similarly pre-processed and stored separately. Reaction time (RT; the time elapsed between target presentation and *t0*) and Movement time (MT; the time between *t0* and the instance when the cursor reached *Target*) were computed to control for variation in movement parameters.

Measures of overall performance

Hand movement error (HME) was calculated as the peak signed perpendicular deviation of the hand trajectory from a straight line connecting the two targets (41). Positive values represent an error in the backward direction (towards the participant's body). As a measure of hand trajectory corrections, absolute peak hand velocity in the anteroposterior direction (HPV) was computed during the movement phase. Signal profiles for a representative participant are shown in **Figure 2** (Left panels - 1st and 2nd line). We performed an additional analysis on the adaptation profiles and adaptation rates of the two groups by considering HME and HPV values during the first block of trials during the adaptation phase (n=54 trials). We chose to fit only the first block of trials, since HME and HPV values reduced rapidly, with values that tend to stabilize after ~40-50 trials. Following each bout of fatiguing exercise, participants showed a slight increase (i.e. sort of forgetting effect) in HME and HPV values for the first trials during re-exposure to perturbation. Individual data were smoothed using a 9-point causal moving average filter and then averaged within each group, similarly to Malone et al., (49). A single-term exponential function was then fitted to each resulting dataset using the following formula in MATLAB:

$$f(x) = b + (c - b)^{-ax}$$

Fitting coefficients were then compared between groups and considered different when their 95% confidence intervals did not overlap.

Measures of postural stability

Center of pressure (CoP) position was computed from GRFs and force plate moments according to Winter (50). CoP position was then demeaned using the mean value of CoP during the first 5 samples of the trial. Maximal backward and forward displacement of the CoP during movement (CoP_{back} and $CoP_{forward}$, respectively) were calculated as the lowest or highest CoP value in the anteroposterior direction (CoP_y trajectory, where negative values represent backward displacement from initial position). CoP anticipatory phase (AP_{CoP}) was quantified as the mean CoP velocity in the anteroposterior direction (CoP_y velocity) over a 150 ms time window starting 100 ms prior- and ending 50 ms after movement onset (*t0*). CoP reactive response (RR_{CoP}) – considered an index of postural corrections (41) – was calculated as the maximum absolute value of CoP_y velocity over the rest of the movement (from 50ms after *t0* until the end of the trial). Calculation windows for AP_{CoP} and RR_{CoP} are shown in the upper right panels of **Figure 2**. Time-windows were based on earlier work (51) and consistent with previous motor adaptation studies (41).

Measures of muscle activation

Linear envelopes of pre-processed EMG signals were computed by applying a 100 Hz low-pass, 4th order, zero-phase digital Butterworth filter. The resulting aligned linear envelopes were then averaged participant-wise across the first/last three consecutive trials for each experimental phase (52), respectively (e.g., for *late baseline* (LB): average of last 3 trials; for *early adaptation* (EA): average of first 3 trials). Concerning *normTrials* – 10 trials where participants had to maintain the hand cursor over a circle-shaped target (1.5 cm radius) and a background constant load of –10 N was applied in the backward direction to activate the muscles – the relative EMG envelopes were averaged across all the trials, yielding a single averaged signal for each muscle.

Phase-averaged EMG signals were then integrated at the level of each muscle using a trapezoidal numerical integration (function "*trapz*" in MATLAB software) for three pre-defined time windows, relative to *t0*: *Anticipatory Phase* (AP) from –150 to +50 ms, *early Reactive Response* (eRR) over a 100 ms window from +50 to +150 ms, and *voluntary Reactive Responses* (vRR) over a 300 ms window from +150 to +450 ms. Time-windows for EMGs integration were chosen based on the nature of the reaching task and on the continuous nature of the force field perturbation. The lower panels of **Figure 2** show a representative muscle in the lower limb (Left TA) and one in the upper limb (AD), respectively. Reactive responses windows differentiate on the physiological nature of the activity: the first window (eRR) mainly represents spinal and supraspinal stretch reflexes responses (53), while vRR conveys information

about voluntary, visually-driven EMG activity ensuring online trajectory correction, which are characterized by longer latencies (~120 to 200 ms in the lower limbs), as shown in previous work (54).

Computed integrals were further normalized for each participant by dividing it by the integral of the averaged EMG activity during *normTrials* ($\int normEMG$; integrated over a 100 ms time-window, starting 100 ms after the force was applied).

$$\mathrm{AP} = \frac{\int_{-100}^{+50} EMG(i)}{\left(\int_{+100}^{+200} normEMG\right) \times 1.5}$$

$$\mathrm{eRR} = \frac{\int_{+50}^{+150} EMG(i)}{\left(\int_{+100}^{+200} normEMG\right) \times 1.5}$$

$$\mathrm{vRR} = \frac{\int_{+150}^{+450} EMG(i)}{\left(\int_{+100}^{+200} normEMG\right) \times 3}$$

We further normalized EMG activity participant-wise by dividing integrated EMG values of each time-window (i.e. AP, eRRs and vRRs) for each experimental phases (i.e. EA, LA_{start}, LA_{end}, EW, LW) by the relative integrated EMG during late baseline (LB) – similarly to (47) – to control for baseline differences and explore changes in muscle activation across phases during APs, eRRs and vRRs.

Finally, we computed indexes of co-activation (C-index) within agonist–antagonist muscle pairs acting at joint level (Left TA/GM, Right TA/GM, Left RF/BF, Right RF/BF and AD/PD) within the framework of the equilibrium-point hypothesis (55). Indices were computed using EMG integrals of ventral and dorsal muscles (before normalization by *late baseline*) for each time-epoch (56–60). Specifically:
If $\int EMG_{ventral}$ and $\int EMG_{dorsal}$ had the same sign:

$$\textit{C-index} = min(|\int EMG_{Ventral}|; |\int EMG_{Dorsal}|)$$

If $\int EMG_{ventral}$ and $\int EMG_{dorsal}$ had opposite sign:

$$\textit{C-index} = 0$$

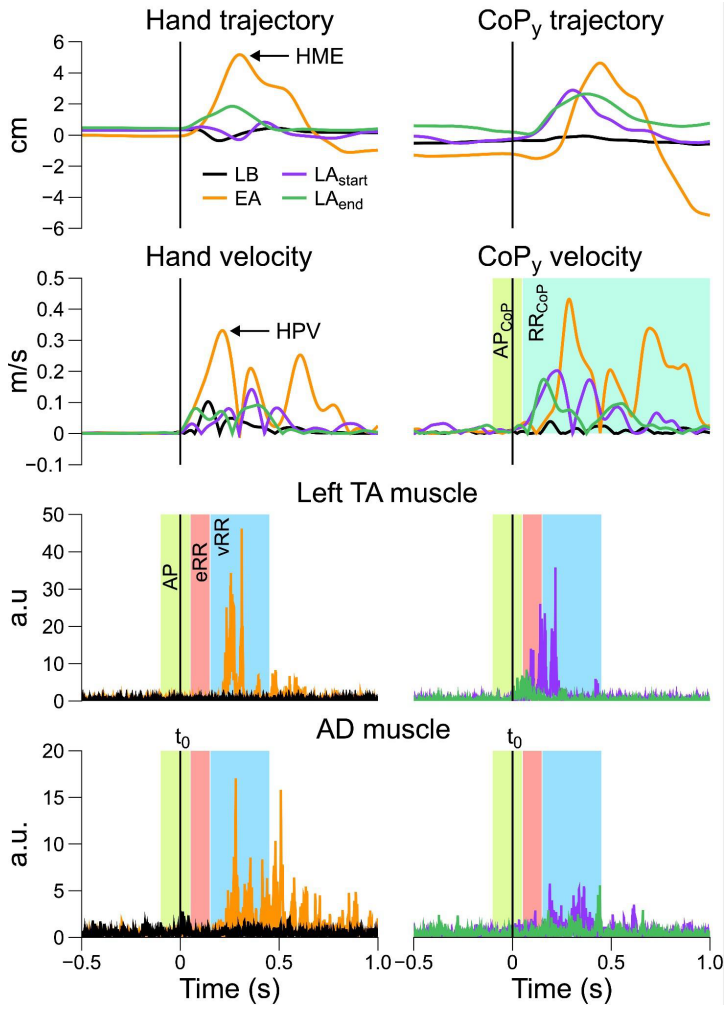

Figure 2
Aligned signals for a representative participant across different experimental phases (different colors - see legend). Vertical black line (t0) corresponds to the hand movement onset. Shaded areas highlight CoP-based and EMG-based calculation windows (see: Data analysis in text). AD: anterior deltoid, AP: anticipatory phase, EA: early adaptation, eRR: early Reactive Response, EW: early washout, HME: hand movement error, HPV: hand peak velocity, LA_{end}: late adaptation – final block, LA_{start}: late adaptation – start, LB: late baseline, LW: late washout, RR: reactive response, TA: tibialis anterior, vRR: voluntary Reactive Response.

Statistical Analysis

Jamovi software (Version 2.3.28; The Jamovi project (2023); https://www.jamovi.org) was used for statistical analyses. All data in the text, Tables, and Figures – unless otherwise stated – are presented as mean ± 1 standard deviation (SD). For all comparisons, statistical significance was set at an α of 0.05. Data distribution (skewness and kurtosis) was assessed, the normality of the data was assessed by the Shapiro–Wilk test and confirmed by the inspection of density and Q–Q plots. When normality assumption was violated, non-parametric statistical tests were performed (Friedman's test with pairwise Durbin-Conover comparisons).

Successively, non-parametric independent samples t-test (Welch-test) was used for pairwise comparisons between groups.

To test the effects of the fatiguing isometric exercise protocol, group differences in MVC changes before and at the end of each bout were assessed using a two-way mixed-design ANOVA (Group–Time).
To test the effects of fatigue on the adaptation process, a two-way mixed-design ANOVA *Group* (Fatigue and No-Fatigue) X *Phase* (LB, EA, LA_{start} and LA_{end} – with *Phase* as a repeated measure factor) was used to assess group differences in performance and postural variables across four experimental phases (LB, EA, LA_{start}, LA_{end}). Assumptions of sphericity were explored using Mauchly's test and controlled for using the Greenhouse–Geisser adjustment in instances where Mauchly's test was significant ($\alpha < 0.05$). The corrected degrees of freedom (DOF) are reported in results. In the event of a significant interaction or main effect, post hoc comparisons were performed using Holm-Bonferroni correction. Non-parametric independent-sample t-tests (Welch-test) were used to assess between-group differences if Levene's test revealed unequal variance.

Similarly, to test the effects of fatigue on the washout process, a two-way mixed-design ANOVA (*Phase* as a repeated measure factor) was used to assess group differences in performance and postural variables across three experimental phases (LB, EW, LW). Integrated EMG time-windows were compared between groups using a two-way mixed-design ANOVA where *Phase* levels were N-1 due to the normalization to LB values (*Phase* as a repeated measure factor). In order to test for differences within each group from LB values, a one-way repeated measure ANOVA (*Phase* as a repeated measure factor) was performed for each group (Fatigue/No-Fatigue), separately.

Results

Our goal here was to evaluate the effects of exercise-induced NMF in the lower extremity on posture stabilization and motor adaptation. We hypothesized that during neuromuscular fatigue (NMF), the central drive to the exercised and unexercised muscles would change to preserve upright postural balance and reaching movement accuracy in a force field adaptation task. To test this hypothesis, we recruited two groups of participants. The first group underwent a submaximal fatiguing protocol to bilaterally fatigue the tibialis anterior muscles. The second group performed the same exercise, but at much lower levels of intensity such that NMF was not induced.

Participants adapted throughout the trials to the introduction of the novel perturbation, both in terms of hand trajectory and in terms of postural measures and muscle activation. As expected, participants in both groups showed appreciable improvement in the reaching task performance, with adaptation strategies persisting even after the removal of the force field perturbation, as shown by the aftereffects –

opposite in direction – on performance in the washout phase (**Figure 3**). NMF caused larger hand movement errors (HME; **Figure 3**) during the adaptation phase for the *Fatigue* group. There were also between-group differences for hand trajectory corrections estimated from hand peak velocity (HPV; **Figure 3**).

Despite the similar results between groups in terms of measures of postural stability (**Figure 6**), muscle activation patterns were affected by NMF (**Figures 4 & 5**). Between-group differences in muscle activation were not limited to the fatigued muscles, but extended to others, non-fatigued and even to upper-limb muscles.

Fatiguing Exercise Produced Significant Reductions in MVC of the Fatigued Muscles

In our study, baseline measurements of maximum voluntary contraction (MVC) isometric ankle dorsiflexion force were comparable between the *Fatigue* Group (264.3 ± 78.2 N) and the *No-Fatigue* Group (261.8 ± 86.1 N), indicating no significant difference in initial strength levels between the groups ($p > 0.05$). The average duration of the isometric fatiguing exercise was 4 mi 15 s (± 2 min,59 s), with an average of 6.6 (± 3.2) cycles. Notably, the duration of exercise decreased across bouts, with the first bout lasting 7 min, 56 s (± 4 min, 14 s) and subsequent bouts showing progressively shorter durations (second bout: 4 min, 4 s ± 1 min , 47 sec, third bout: 3 min, 30 s ± 1 min , 41 s, fourth bout: 3 min, 19 sec ± 1 min, 37 s, fifth bout: 2 min, 27 s ± 1 min , 58 s). Following the fatiguing exercise, a significant reduction in MVC isometric force was observed exclusively in the Fatigue (-32 ± 4%), compared to the No-Fatigue (1 ± 3%) group, indicating a pronounced effect of the isometric fatiguing exercise on muscle force in the fatigue condition ($p < 0.001$).

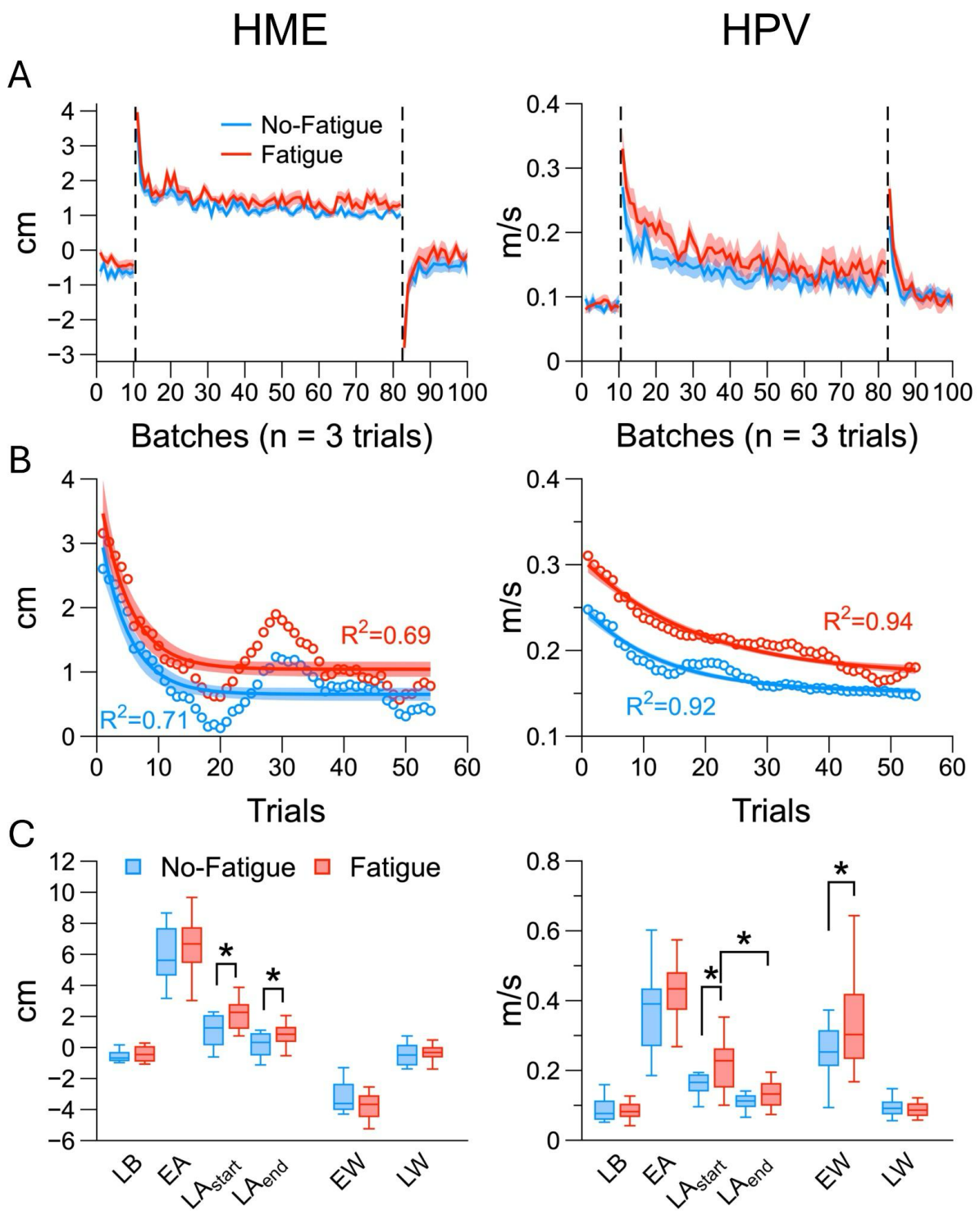

Figure 3.

Overall performance variables during the reaching task divided by group. A) Batch-averaged curves for hand movement error (HME; left panel) and hand peak velocity (HPV; right panel) throughout the experimental phases. Positive HME values represent a backward error (towards the participant). HPV was computed in absolute values. Vertical dotted lines represent the transition across experimental phases (baseline, adaptation, washout). Data are averaged in batches of n=3 trials and reported as mean (thick lines) ± 1 Standard Error (SE; shaded areas). B) Fitting curves (thick lines) and confidence intervals (C.I.) of the fittings (shaded areas) for HME (left) and HPV (right) group-averaged values (circles) during

*the first block of adaptation trials. C) Box plots for HME (left) and HPV (right) values across the considered experimental phases. Boxes depict data from first to third quartile, whiskers represent minimum and maximum data points. Median is shown by the horizontal line. * significant effects ($p < 0.05$) between groups. EA: early adaptation, EW: early washout, LA_{end}: late adaptation – final block, LA_{start}: late adaptation – start, LB: late baseline, LW: late washout.*

Reaching Performance Exhibited Phase Dependent Adaptive Changes and the Fatigue Group Adapted Slower Than the No-Fatigue Group

We measured reaching movement performance by measuring HME, the peak signed perpendicular deviation of the hand trajectory from a straight line connecting the two targets, and the peak hand velocity in the anteroposterior direction, HPV. Note that since the intended movement was along the medial-lateral direction, we expected HPV to be very small for baseline blocks and return to almost zero values late in the adaptation.

HME and HPV exhibited a decline across both the Fatigue and No-Fatigue groups during the adaptation task, as shown in **Figure 3A**. Additional analyses were performed considering HME and HPV group-averaged data during the first adaptation block (see Methods). The fitting lines described quite well the HME dataset, as indicated by goodness of fit parameters (adj R^2=0.69 and 0.72; RMSE= 0.34 and 0.3 for Fatigue and No-Fatigue, respectively). Fitting coefficients *a* and *c* were similar between the groups (Fatigue: 0.21 [0.13 – 0.29], No-Fatigue: 0.21 [0.14 – 0.29]; Fatigue: 4.03 [3.22 – 4.83], No-Fatigue: 3.48 [2.76 – 4.20], respectively). Coefficient *b* was higher in the Fatigue group (Fatigue: 1.04 [0.93 – 1.16], No-Fatigue: 0.65 [0.55 – 0.75]), confirming the higher steady-state final value (**Figure 3**, **B** - left side).

Fitting lines for HPV values described quite well the dataset, as indicated by goodness of fit parameters (adj R^2=0.94 and 0.92; RMSE= 0.01 and 0.01 for Fatigue and No-Fatigue, respectively). Despite a small difference in coefficient *a*, the confidence intervals for the slope of the fittings did not differ between the groups (Fatigue: 0.055 [0.042 – 0.067], No-Fatigue: 0.078 [0.062 – 0.094]. The other two fitting coefficients, *b* (F: 0.171 [0.161 0.18], No-Fatigue: 0.151 [0.147 – 0.156]) and *c* (Fatigue: 0.307 [0.297 – 0.318], No-Fatigue: 0.252 [0.242 – 0.262]) were higher for the Fatigue group, denoting both a higher initial value and a higher steady-state final value for HPV in the Fatigue group (**Figure 3**, **B** - right side).

Considering that most of our data did not meet normality assumption, a non-parametric statistical model was employed (i.e. Friedman's test for repeated measures) to test for factor Phase (*LB*: Late Baseline, *EA*: Early Adaptation, LA_{start}: Start of Late Adaptation, and LA_{end}: End of Late Adaptation). We observed a significant main effect of Phase on HME (χ^2 (3) = 73.6, $p < 0.001$), which differed across all pairwise comparisons ($p < 0.001$). **Figure 3C** illustrates a sharp increase

in HME transitioning from *LB* to *EA*, followed by a gradual decrease throughout the adaptation phase.

Conversely, during the washout phase, an initial negative trend in HME was observed, which subsequently approached values near zero towards the end of adaptation. This pattern was statistically confirmed by examining Phase effects, with early washout (EW) and late washout (LW) as specific intervals. A repeated measures ANOVA revealed a significant main effect for Phase ($F_{(1.35, 35.22)} = 194.26$, $p < 0.001$), underscoring the dynamic changes in HME over the course of the study.

To test the effect of Fatigue, we performed non-parametric independent samples of Welch's t-test to compare between Fatigue and No-Fatigue groups in each Phase. The test showed a statistically significant difference in HME between groups both at LA_{start} (Fatigue: 2.06 ± 0.93 No-Fatigue: 1.08 ± 0.98; t (-2.739) = 25.9, p = 0.011, Cohen's *d* = 1.035) and at LA_{end} phases (Fatigue: 0.85 ± 0.77 No-Fatigue: 0.17 ± 0.74; t (25.9) = -2.385, p = 0.025, *d* = 0.902), where HME was higher in the Fatigue group.

HPV exhibited a pattern throughout the experiment that paralleled HME. The influence of the experimental phase on HPV was statistically significant (χ^2 (3) = 65.2, $p < 0.001$), while the reduction in HPV values from the start (LA_{start}) to the end (LA_{end}) of the late adaptation phase was significant only for the Fatigue group. Welch's t-test conducted during the adaptation phase revealed a significant difference in HPV between the two groups at the start (LA_{start}) of the late adaptation phase, with the Fatigue showing higher HPV (0.21 ± 0.08) compared to the No-Fatigue (0.16 ± 0.05; t = -2.296, p = 0.003, *d* = 0.87, as illustrated in **Figure 3**, **C**).

Similarly, during the washout phase, HPV continued to follow the trend observed during the adaptation phase. A significant main effect for Phase was noted (χ^2 (2) = 42.3, $p < 0.001$), and a Welch's t-test identified a significant difference in HPV between the groups at the early washout (*EW*) phase, with the Fatigue displaying higher HPV values (0.33 ± 0.13) compared to the No-Fatigue group (0.24 ± 0.09; t = -2.1206, p = 0.045, *d* = 0.8, as shown in **Figure 3**, **C**).

Neuromuscular Fatigue Induced Changes in Muscle Activity Occurred Mainly in Upper Extremity Muscles and Left Side of the Lower Body

Effects of NMF were more evident on the left-side of the body and effector (i.e. shoulder) muscles. Notable changes in EMG patterns were seen across the adaptation experimental phases (*EA*, LA_{start} and LA_{end}; **Figure 4**) in both groups. Significant differences in muscle activation compared to *LB* phase ($p < 0.05$) were also present and are illustrated in **Figure 4** and **Supplemental material (S1–S3)** using the arrow symbol below the box plots.

In detail, across each time-window (AP, eRR, vRR) we observed higher *anterior deltoid* (AD) muscle activity in the Fatigue compared to the No-Fatigue group (**Figure 4**), first row; **Table 1**). Compared to baseline (*LB)* values, AD activity increased across all time windows, especially in the Fatigue group (bottom arrow symbols in **Figure 4**, first row). EMG activation of left *tibialis anterior* and *rectus femoris* muscles (**Figure 4**, 2nd and 3rd row; and **Table 1**) generally increased across experimental phases. In contrast to the AD muscle, where the Fatigue group showed higher activation, EMG activation was generally higher in No-Fatigue compared to the Fatigue group for left TA and left RF. Overall, we observed a reduction in EMG activation for each muscle across the experimental phases during vRR. The statistical results are summarized in Table 1. Supplementary results during the *adaptation* phase for the other muscles are reported in Supplementary materials (**S1** and **S2**).

Results for the *washout* phase partially reflect the typical aftereffects seen in the performance variables, with EMG values slowly returning to values close to late baseline (*LB)*. Significant differences between groups are appreciable in AP, eRR and vRR windows in both upper- and lower-limb muscles.

Overall, the aftereffects were similar to the adaptation phase results. We observed increased AD activation for the Fatigue group, especially during eRR window, while activation of left TA and RF muscles was higher in the No-Fatigue group during the same window. The washout results are summarized in Table 1. Detailed results for the *washout* phase are reported in Supplementary materials (**S1, S2** and **S3**)

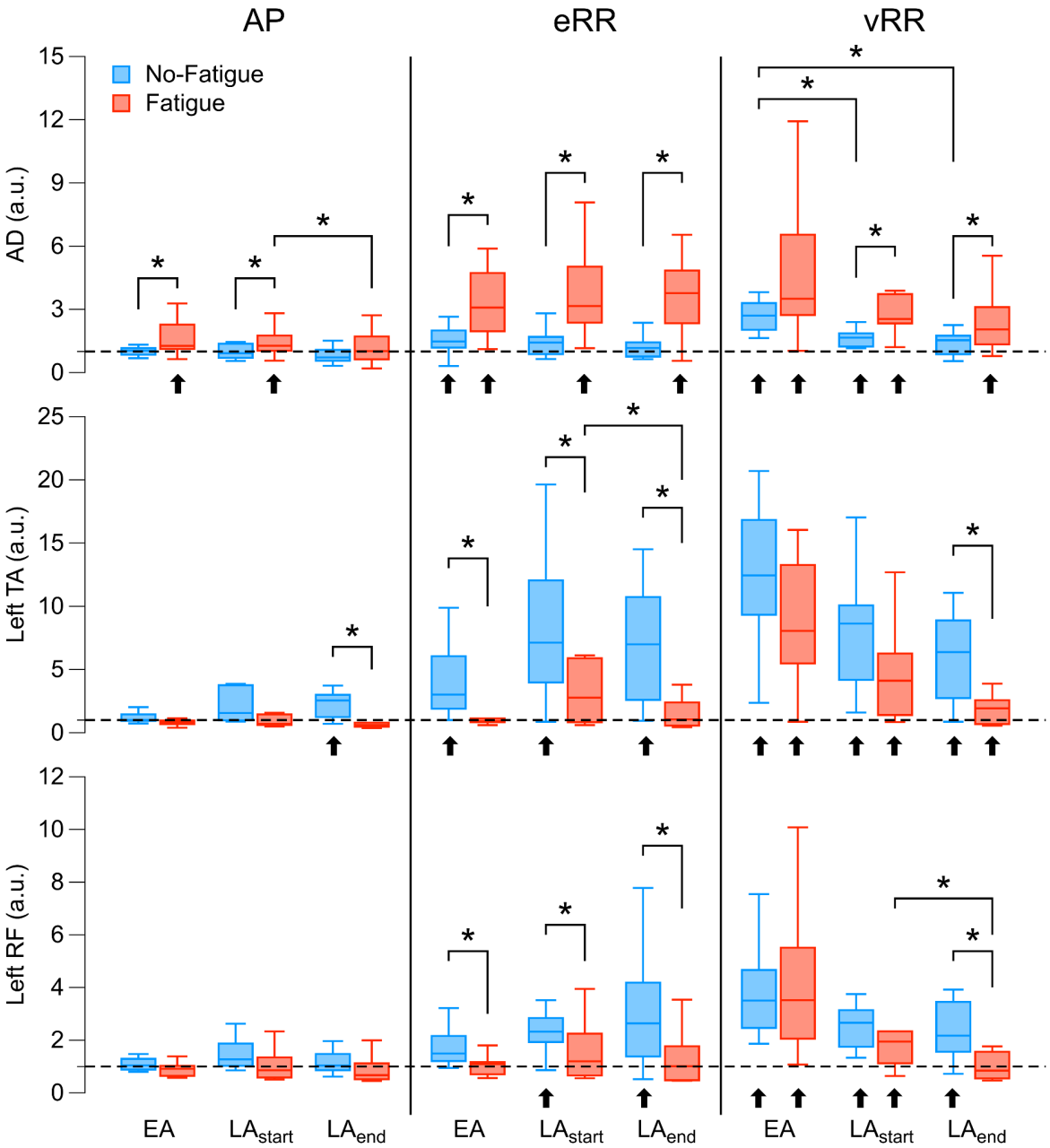

Figure 4.

*EMG activity of individual muscles for each predetermined time window across the learning phase. Muscles are reported on different lines, while EMG time-windows are placed side-by-side in chronological order. Box plots between the 25th and 75th quartiles and the whisker showing the min and max values with median values (thick horizontal lines) are presented. Values are normalized participant-wise to the LB values and reported in arbitrary units (a.u.). * significant between/within group effects ($p < 0.05$); ⬆ significant difference from LB ($p < 0.05$). Black horizontal dashed line =1 represents LB values. AD: anterior deltoid, AP: anticipatory phase, BF: biceps femoris, EA: early adaptation, eRR: early Reactive Response, EW: early washout, GM: gastrocnemius medialis, LA_{end}: late adaptation – final block, LA_{start}: late adaptation – start, LB: late baseline, LW: late washout, PD: posterior deltoid, RF: rectus femoris, TA: tibialis anterior, vRR: voluntary Reactive Response.*

Adaptation Phase

Muscle	AP		eRR		vRR	
	Factor	***P*-Value (Post-hoc)**	**Factor**	***P*-Value (Post-hoc)**	**Factor**	***P*-Value (Post-hoc)**
AD	*Group*	**EA** ($p < 0.05$ $d = 0.79$) **LA_{start}** ($p < 0.05$ $d = 0.86$)	*Group*	**EA** ($p < 0.001$ $d = 1.44$) **LA_{start}** ($p < 0.05$ $d = 0.98$) **LA_{end}** ($p < 0.01$ $d = 1.52$)	*Group*	**LA_{start}** ($p < 0.05$ $d = 1.05$) **LA_{end}** ($p < 0.05$ $d = 0.9$)
	Phase	$\chi^2(2) = 15.4$ **$p < 0.001$** ***Fatigue only*: LA_{start} - LA_{end}** ($p<0.01$)	*Phase*	n.s.	*Phase*	***No-Fatigue only***: $\chi^2(2) = 16.2$ **$p < 0.05$** **EA–LA_{start}** ($p < 0.001$) **EA–LA_{end}** ($p < 0.001$)
Left TA	*Group*	**LA_{end}** ($p < 0.05$ $d = -0.92$)	*Group*	**EA** ($p < 0.01$ $d = -1.11$) **LA_{start}** ($p < 0.05$ $d = -0.85$) **LA_{end}** ($p < 0.01$ $d = -1.23$)	*Group*	**LA_{start}** ($p = 0.058$ $d = -0.75$) **LA_{end}** ($p < 0.01$ $d = -1.31$)
	Phase	$\chi^2(2) = 42.7$ **$p < 0.001$**	*Phase*	***Fatigue only:*** $\chi^2(2) = 6.14$ **$p < 0.05$** **LA_{start}–LA_{end}** ($p < 0.05$)	*Phase*	$\chi^2(2) = 42.7$ **$p < 0.001$**
Left RF	*Group*	n.s.	*Group*	**EA** ($p < 0.05$ $d = -0.9$) **LA_{start}** ($p < 0.05$ $d = -0.82$) **LA_{end}** ($p < 0.05$ $d = -1.04$)	*Group*	**LA_{end}** ($p < 0.01$ $d = -1.28$)
	Phase	n.s.	*Phase*	$\chi^2(2) = 7.36$ **$p < 0.05$** **EA–LA_{start}** ($p < 0.01$)	*Phase*	$\chi^2(2) = 31.7$ **$p < 0.001$** ***Fatigue only*: LA_{start}– LA_{end}** ($p < 0.001$)

Washout Phase

Muscle	AP		eRR		vRR	
	Factor	***P*-Value (Post-hoc)**	**Factor**	***P*-Value (Post-hoc)**	**Factor**	***P*-Value (Post-hoc)**
AD	*Group*	n.s.	*Group*	**EW** ($p < 0.01$; $d = 1.39$)	*Group*	**EW** ($p < 0.05$; $d = 0.84$)
	Phase	$\chi^2(1) = 5.54$ **$p < 0.05$**	*Phase*	***Fatigue only:*** $\chi^2(1) = 7.14$ **$p < 0.001$**	*Phase*	***Fatigue only***: $\chi^2(1) = 7.14$ **$p < 0.001$**
Left TA	*Group*	**LW** ($p < 0.001$; $d = -1.42$)	*Group*	**EW** ($p<0.05$; $d = -0.88$) **LW** ($p<0.01$; $d = -1.15$)	*Group*	**LW** ($p < 0.05$; $d = -0.91$)
	Phase	n.s.	*Phase*	***No- Fatigue only:*** $\chi^2(1) = 9.31$ **$p < 0.001$**	*Phase*	$\chi^2(1) = 13.4$ **$p < 0.001$**
Left RF	*Group*	**EW** ($p < 0.05$; $d = -0.95$) **LW** ($p < 0.01$; $d = -1.36$)	*Group*	**EW** ($p < 0.05$; $d = -1$) **LW** ($p < 0.001$; $d = -1.43$)	*Group*	**EW** ($p < 0.008$; $d = -1.13$) **LW** ($p = 0.001$; $d = -1.35$)
	Phase	$\chi^2(1) = 11.6$ **$p < 0.001$**	*Phase*	$\chi^2(1) = 11.6$ **$p < 0.001$**	*Phase*	$\chi^2(1) = 5.14$ **$p < 0.05$**

Table 1: *Statistical analysis results for considered EMG windows (anticipatory phase (AP – 1st column), early reactive response (eRR – 2nd column), voluntary reactive response (vRR – 3rd column)) of anterior deltoid (AD), left tibialis anterior (Left TA) and left rectus femoris (Left RF) muscles. d= Cohen's d (effect size)*

Similarly to EMG amplitudes of individual muscles, NMF affected mainly the co-activation index (C-index) at the level of the shoulder and the left leg.
In detail, co-contraction between the anterior deltoids (AD) and posterior deltoids (PD) increased during adaptation, especially in the Fatigue group. During the voluntary Reactive Response (vRR) window C-index increased similarly in both groups following the introduction of the perturbation (*EA*) and later decreased approaching values close to late baseline (*LB*) at the end (LA_{end}) of the adaptation phase (**Figure 5**, first row).

C-index for left TA-GM and RF-BF muscle pairs was higher in the No-Fatigue group across the adaptation phase during each window. C-index demonstrated an increasing trend across adaptation during both anticipatory phase (AP) and early Reactive Response (eRR) windows, especially for the No-Fatigue group. During vRR, C-index showed a decreasing trend, mainly for the left TA-GM muscle pair (**Figure 5**, 2nd and 3rd row; **Table 2**).

The C-index of right-side muscle pairs increased across the adaptation phase, especially in the No-Fatigue group. Differences between groups, however, were less evident (see Supplementary Materials, **S4**).

Trends for C-index during washout phase were similar to individual EMGs results and demonstrate an after-effect following the removal of the perturbation during early washout (*EW*). Aftereffects in AD-PD muscle pair C-index were significant only for the Fatigue group. The C-index of left TA-GM and RF-BF muscle pairs showed increased values in the No-Fatigue compared to the Fatigue group. C-index similarly decreased in both groups from *EW* to *LW* (see Supplementary Materials, **S5**).

Unlike EMG amplitudes that primarily changed on the left side of the body, C-index of right-side muscle pairs highlighted group differences only for RF-BF at *LW* during the anticipatory phase, and close to significance for *EW*. Overall, the decrease in C-index across the washout phase was significant mainly in the Fatigue group (see Supplementary Materials, **S4**).

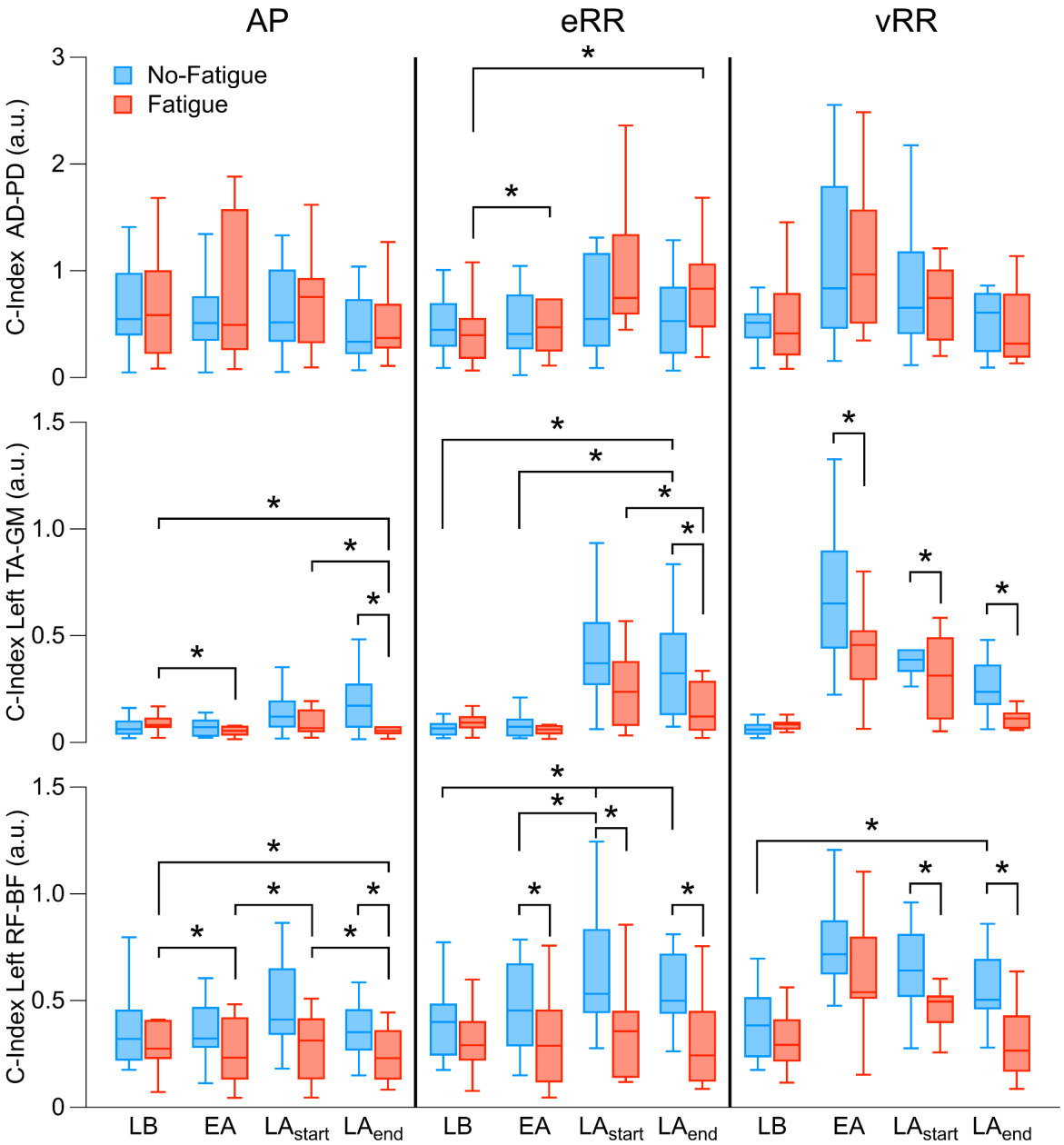

Figure 5.

*Co-activation index (C-index) at the level of agonist-antagonist muscle pairs across the learning phase. Muscle pairs are reported on different lines, while EMG time-windows are placed side-by-side in chronological order. Box plots between the 25th and 75th quartiles and the whisker showing the min and max values with median values (thick horizontal lines) are presented. Values are normalized participant-wise and reported in arbitrary units (a.u.). * significant between/within group effects ($p < 0.05$). AD: anterior deltoid, AP: anticipatory phase, BF: biceps femoris, EA: early adaptation, eRR: early Reactive Response, EW: early washout, GM: gastrocnemius medialis, LA_{end}: late adaptation – final block, LA_{start}: late adaptation – start, LB: late baseline, LW: late washout, PD: posterior deltoid, RF: rectus femoris, TA: tibialis anterior, vRR: voluntary Reactive Response.*

Adaptation Phase

Muscle pair	AP		eRR		vRR	
	Factor	***P*-Value (Post-hoc)**	**Factor**	***P*-Value (Post-hoc)**	**Factor**	***P*-Value (Post-hoc)**
AD-PD	*Group*	n.s.	*Group*	n.s.	*Group*	n.s.
	Phase	$\chi^2(3) = 8.74$ $p < 0.05$ **LB–LA$_{end}$** ($p = 0.057$) **EA–LA$_{end}$** ($p = 0.057$) **LA$_{start}$–LA$_{end}$** ($p < 0.01$)	*Phase*	$\chi^2(3) = 23.7$ $p < 0.001$ All: **LB–LA$_{start}$; EA–LA$_{start}$** ($p < 0.001$) ***Fatigue only:*** **LB–EA;** ($p < 0.05$) **LB–LA$_{end}$** ($p < 0.001$)	*Phase*	$\chi^2(3) = 42.7$ $p < 0.001$ **LB–EA; LB–LA$_{start}$; LA$_{start}$–LA$_{end}$; EA–LA$_{end}$** ($p < 0.001$) **EA– LA$_{start}$** ($p < 0.05$)
Left TA-GM	*Group*	**LA$_{end}$** ($p < 0.05$ $d = 0.84$)	*Group*	**LA$_{end}$** ($p < 0.05$ $d = 1.05$)	*Group*	**EA** ($p < 0.05$ $d = 0.86$) **LA$_{start}$** ($p < 0.05$ $d = 0.88$) **LA$_{end}$** ($p < 0.05$ $d = 1.07$)
	Phase	***Fatigue only:*** $\chi^2(3) = 11.2$ **$p < 0.05$** **LB–EA; LA$_{start}$–LA$_{end}$** ($p < 0.05$) **LB–LA$_{end}$** ($p < 0.001$)	*Phase*	$\chi^2(3) = 28.9$ **$p < 0.001$** ***Fatigue only:*** **LA$_{start}$ –LA$_{end}$** ($p < 0.05$) ***No-Fatigue only:*** **LB–LA$_{end}$** ($p < 0.01$) **EA–LA$_{end}$** ($p < 0.001$)	*Phase*	$\chi^2(3) = 55.2$ **$p < 0.001$** **LB–LA$_{end}$** ($p < 0.05$) All other comparisons ($p < 0.001$)
Left RF-BF	*Group*	**LA$_{end}$** ($p < 0.05$ $d = 1.02$)	*Group*	**EA** ($p < 0.05$ $d = 0.82$) **LA$_{start}$** ($p < 0.05$ $d = 0.9$) **LA$_{end}$** ($p < 0.01$ $d = 1.11$)	*Group*	**LA$_{start}$** ($p < 0.05$ $d = 0.94$) **LA$_{end}$** ($p < 0.001$ $d = 1.53$)
	Phase	***Fatigue only:*** $\chi^2(3) = 9.69$ **$p < 0.01$** **LB–EA; LB–LA$_{end}$; EA– LA$_{start}$; LA$_{start}$–LA$_{end}$** ($p < 0.05$)	*Phase*	***No-Fatigue only:*** $\chi^2(3) = 10.5$ **$p < 0.05$** **LB– LA$_{start}$** ($p < 0.001$) **LB–LA$_{end}$; EA– LA$_{start}$** ($p < 0.05$)	*Phase*	$\chi^2(3) = 40.5$ **$p < 0.001$** **LB–EA; LB–LA$_{start}$; EA–LA$_{end}$; LA$_{start}$–LA$_{end}$** ($p < 0.001$) ***No-Fatigue only:*** **LB–LA$_{end}$** ($p < 0.05$)

Washout Phase

Muscle pair	AP		eRR		vRR	
	Factor	***P*-Value (Post-hoc)**	**Factor**	***P*-Value (Post-hoc)**	**Factor**	***P*-Value (Post-hoc)**
AD-PD	*Group*	n.s.	*Group*	n.s.	*Group*	n.s.
	Phase	$\chi^2(2) = 6.64$ **$p < 0.05$** **LB–LW; EW–LW** ($p < 0.05$)	*Phase*	***Fatigue only:*** $\chi^2(2) = 13$ **$p < 0.01$** **LB–EW; EW–LW** ($p < 0.001$)	*Phase*	***Fatigue only:*** $\chi^2(2) = 8.71$ **$p < 0.05$** **LB–EW; EW–LW** ($p < 0.01$)
Left TA-GM	*Group*	n.s.	*Group*	**EW** ($p < 0.05$ $d = 0.92$)	*Group*	n.s.
	Phase	$\chi^2(2) = 15.6$ **$p < 0.001$** **LB–LW; EW–LW** ($p < 0.001$)	*Phase*	$\chi^2(2) = 23.8$ **$p < 0.001$** **LB–LW; EW–LW** ($p < 0.001$)	*Phase*	$\chi^2(2) = 32.4$ **$p < 0.001$** **LB–EW** ($p < 0.01$) **LB–LW; EW–LW** ($p < 0.001$)
Left RF-BF	*Group*	**EW** ($p < 0.05$ $d = 0.87$) **LW** ($p < 0.05$ $d = 0.95$)	*Group*	**EW** ($p < 0.01$ $d = 1.28$) **LW** ($p < 0.001$ $d = 1.41$)	*Group*	**EW** ($p < 0.01$ $d = 1.12$) **LW** ($p < 0.01$ $d = 1.1$)
	Phase	$\chi^2(2) = 19.9$ **$p < 0.001$** **LB–LW; EW–LW** ($p < 0.001$) ***Fatigue only:*** **LB–EW** ($p < 0.01$)	*Phase*	$\chi^2(2) = 23.6$ **$p < 0.001$** **LB–LW; EW–LW** ($p < 0.001$)	*Phase*	***Fatigue only:*** $\chi^2(2) = 17.3$ **$p < 0.001$** **LB–LW** ($p < 0.001$) **LB–EW; EW–LW** ($p < 0.01$)

Table 2: *Statistical analysis results for muscle-pairs coactivation index (C-index) in the considered windows (anticipatory phase (AP – 1st column), early reactive response (eRR – 2nd column), voluntary reactive response (vRR – 3rd column)) for anterior deltoid – posterior deltoid (AD-PD), left tibialis anterior – gastrocnemius medialis (Left TA-GM) and left rectus femoris – biceps femoris (Left RF-BF) muscle pairs. d= Cohen's d.*

Center-of-Pressure Excursion is Stabilized during Neuromuscular Fatigue
During the early adaptation phase, the center of pressure shifted more towards the back in the Fatigue group, as shown in **Figure 6A**. Aside from that, the displacement of the center of pressure was similar between the two groups. Statistical results for measures of postural stability across experimental phases are shown in **Figure 6B**. Repeated measures ANOVA revealed a main effect of *Phase* on $CoP_{forward}$ ($F_{(2.03, 52.81)} = 33.10$, $p < 0.001$, $\eta^2 = 0.393$). Holm-Bonferroni post hoc pairwise tests indicated values were different across each condition ($p < 0.05$) except for LA_{start}–LA_{end} comparison. A main effect of *Phase*Group* interaction was also found ($F_{(2.03, 52.81)} = 3.48$, $p = < 0.037$, $\eta^2 = 0.041$). Holm-Bonferroni post hoc pairwise tests indicated values at EA were significantly higher for No-Fatigue ($p = 0.036$; **Figure 6**, **B** – top panel).

A main effect of *Phase* was found for CoP_{back} ($F_{(2.23, 55.73)} = 171.95$, $p = < 0.001$, $\eta^2 = 0.766$), where Holm-Bonferroni post hoc pairwise comparisons were significant for each condition ($p < 0.001$; $p = 0.012$ for LA_{start}–LA_{end}). *Phase* effect was found also for APC ($F_{(1.93, 48.36)} = 4.7$, $p = 0.048$, $\eta^2 = 0.093$), where Holm-Bonferroni post hoc pairwise comparisons revealed statistical differences only between LB–LA_{start} and LB–LA_{end} comparisons (LB: 0.0115 ± 0.005: LA1 0.0177 ± 0.012; LAend: 0.205 ± 0.017; $p = 0.045$). Finally, a *Phase* effect was confirmed also for RCP ($F_{(1.9, 47.61)} = 82.8$, $p < 0.001$, $\eta^2 = 0.589$). Holm-Bonferroni post hoc pairwise comparisons were significant for each condition ($p < 0.05$). Despite the visually appreciable modifications in CoP_y profiles across phases (**Figure 6**, **A**), there were no significant effects of *Group* and *Phase*Group* interaction in both *learning* and *washout* phases on measures of postural stability – except for $CoP_{forward}$ at EA (**Figure 6**, **B**). Results for CoP variables during the *washout* phase are reported in Supplementary materials (**S6**).

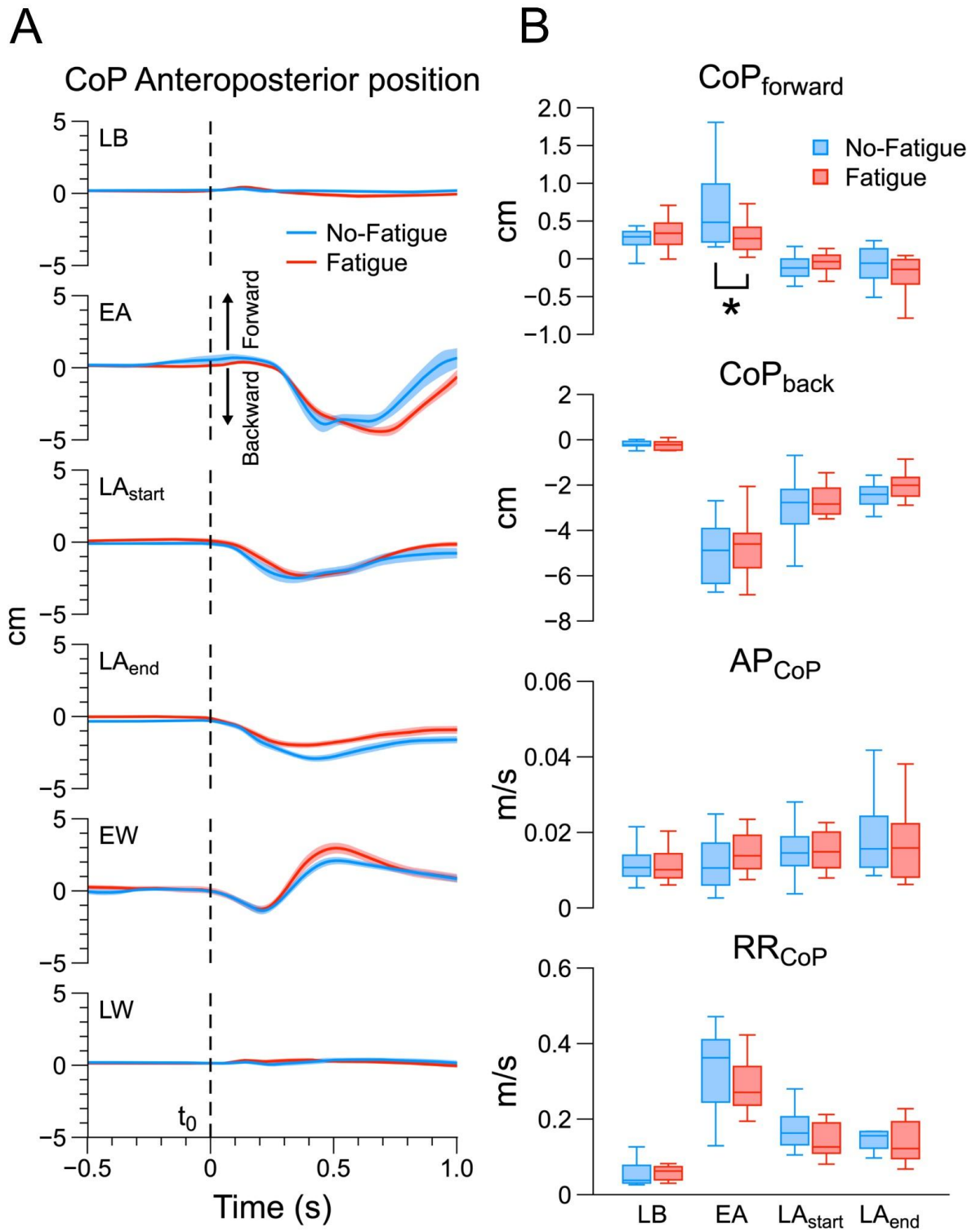

Figure 6.
A: *Group-averaged CoP_y trajectory aligned at movement onset (t0) across experimental phases. Thick lines represent means and shaded areas depict ± 1 Standard Error (SE). Vertical dashed lines represent hand movement onset (t0). Forward (positive) and backward (negative) displacement are indicated by the thick black arrows.* **B:** *Measures of postural stability across the learning phase. * significant between/within group effects ($p < 0.05$). Individual data points (dots and diamonds) with median values (black horizontal lines) are*

presented. First panel ($CoP_{forward}$): maximal forward displacement of CoP during the reaching movement; Second panel (CoP_{back}): maximal backward displacement of CoP during the reaching movement; Third panel (anticipatory postural control – APC): mean CoP_y velocity during anticipatory phase; Fourth panel (reactive control of posture – RCP): peak CoP_y velocity during the movement.EA: early adaptation, EW: early washout, LA_{end}: late adaptation – final block, LA_{start}: late adaptation – start, LB: late baseline, LW: late washout.

Discussion

In this study, we examined how localized neuromuscular fatigue (NMF) in the tibialis anterior, a key postural muscle, influences the adaptive mechanisms necessary for performing human reaching movements while standing upright. We employed a force field perturbation paradigm as our experimental approach to investigate the processes of motor adaptation. Our findings revealed that postural control metrics did not change following exercises that induced fatigue, supporting our initial hypothesis that individuals would prioritize maintaining their posture to aid in performing reaching tasks. This prioritization was achieved through bilateral adjustments in muscle activity, both in muscles subjected to fatiguing exercises and those that were not.

The study also demonstrated that NMF adversely affected the ability to execute reaching movements during both the initial and final phases of adaptation to the force field, identified as LA_{start} and LA_{end} phases, respectively. This result highlighted that fatigue led to greater errors in movement during these phases, though it did not alter the rate of adaptation. Furthermore, we observed differences in the activation patterns of individual muscles and the co-activation patterns of muscle pairs among participants. These differences indicate that the group experiencing fatigue employed unique strategies, likely indicative of a central adaptation mechanism, to mitigate the impact of NMF on the tibialis anterior muscles.

Upright Postural Control Following Localized NMF

We monitored both anticipatory and reactive postural adjustments in participants across two cohorts—those experiencing localized neuromuscular fatigue (Fatigue) and those without fatigue (No-Fatigue)—when exposed to force field disturbances. Anticipatory responses, which are preparatory adjustments made before the commencement of reaching tasks, and reactive responses, immediate adjustments in response to postural perturbations, were observed in participants of both groups. This finding is in agreement with earlier studies (41, 46), suggesting a similar adaptation in postural control strategies under similar experimental conditions.

Significantly, our study revealed a dynamic change in postural stability metrics over time, particularly in terms of the Center of Pressure's (CoP) displacement or velocity in the anteroposterior direction, as illustrated in **Figure 6**. Despite these temporal changes, we did not detect significant differences in postural stability between the

Fatigue and No-Fatigue groups. Over time, there was a notable reduction in the reactive response of the CoP (RR_{CoP}), indicating improvements in online postural corrections, alongside an increase in anticipatory postural control of the CoP (AP_{CoP}). This suggests that participants in both groups efficiently developed motor strategies to preemptively counteract and adapt to the disturbances caused by the force field perturbation, enhancing postural stability.

These adaptive behavioral responses are supported by findings from studies that examined the impact of intentional, specific movements of the upper limbs on postural stability (4–6). For example, Strang and colleagues documented modifications in the timing of muscle activation in response to neuromuscular fatigue, affecting both fatigued and non-fatigued muscles (7). Such adjustments in muscle activation demonstrate the central nervous system's (CNS) involvement, particularly supraspinal structures, in modifying neural signals to various muscles. The purpose of this adjustment is to preserve postural stability during the performance of tasks that require precision with the upper limbs, underscoring the CNS's critical function in orchestrating and harmonizing motor responses across the body to maintain balance and posture.

The findings of Strang and colleagues are congruent with our observations concerning muscle activation patterns. Despite identifying differences in activation at both the level of individual muscles (**Figure 4**) and in the coordinated activation of muscle pairs (**Figure 5**), we observed no alterations in postural stability following fatiguing exercises. This finding is echoed in the work of Singh and Latash, who also noted no significant shifts in the Center of Pressure (CoP) during voluntary sway tasks performed while standing, even after fatigue had modified patterns of muscle activation and muscle synergies (17). Furthermore, a more recent study revealed that although exercises targeting the soleus muscle altered EMG activity parameters, they did not affect balance performance in dynamic postural tasks (26). These outcomes suggest that in the context of complex motor tasks, such as maintaining an upright posture which necessitates the involvement of multiple joints and muscles (61, 62), the central nervous system (CNS) implements compensatory strategies to ensure the stabilization of motor performance during fatigue (7).

It is important to note that the assessment of neuromuscular fatigue (NMF)-induced effects on postural control is influenced by a variety of factors that could potentially confound the results (61, 62). These include the duration and modality of exercise (62), as well as the specific anatomical location of NMF (61). Despite a substantial body of research exploring the impact of NMF on postural control—a comprehensive review can be found in (61)—the majority of studies have primarily concentrated on the short-term, transient effects of NMF (6, 7, 22, 27). Conversely, other research has evaluated postural control during the recovery period following acute high-intensity whole-body exercise (63) or isometric localized exercise (64, 65). However, interpreting these findings is complex due to the multitude of physiological responses

involved both during the exercise (62, 66) and in the subsequent recovery phase (67).

In our study, we designed a fatiguing protocol that induced a prolonged state of fatigue. This protocol was repeated to maintain a sustained level of fatigue, deliberately interfering with the natural, time-dependent physiological recovery processes (67). Furthermore, it is noteworthy that most previous tasks employed in this research area involved volitional movements or the countering of predictable perturbations, with which participants were already acquainted (6, 7, 23, 24). This familiarity presents challenges in accurately assessing the dynamics of adaptation and the specific influence of NMF on these processes.

Fatigue-induced effects on reaching performance in a force field during upright stance

The performance in reaching tasks, quantified by hand movement error (HME) — the maximum deviation of the hand's path from a straight line between targets — demonstrated a trend of exponential decrease, as illustrated in **Figure 3A**. This observation is consistent with findings from similar research on motor adaptation in reaching tasks conducted in a standing position (41, 46, 47).

In this study, the impact of neuromuscular fatigue (NMF) on hand movement error (HME) and hand peak velocity (HPV) were significant across some experimental phases. Although the adaptation phase showed a reduction in HME and HPV comparable to that seen in non-fatigued conditions (**Figure 3**, **A**), and similar patterns of aftereffects were observed after perturbation removal (washout phase), the Fatigue group experienced an altered adaptation process for both the variables. This was evident from elevated HME and HPV values at the conclusion of both the first block and the entire adaptation phase (**Figure 3**, **C**).

We interpret the dynamics of reaching behavior during fatigue within the framework of the two-stage model of motor adaptation: an early phase characterized by rapid learning followed by quick decline, and a later phase marked by slower acquisition but with prolonged retention (68). It has been proposed that these fast and slow learning phases correspond to explicit and implicit learning processes, respectively (69). From a computational perspective, explicit learning is geared towards achieving specific goals, whereas implicit learning focuses on the precise execution of movements (70). This distinction is mirrored in the underlying neural mechanisms: strategies for target acquisition, which are employed to counter experimentally induced disturbances, are governed by prefrontal cortex activity. In contrast, implicit learning depends on the cerebellum (71–76), with proprioception playing a key role in driving implicit learning (77, 78).

Studies have shown that neuromuscular fatigue (NMF) can deteriorate proprioceptive sensitivity, leading to diminished joint position awareness, impaired coordination, and decreased proprioceptive accuracy (see (79, 80) for a review). Our observations of reduced movement correction during late stages of adaptation in a fatigued state might be attributed to the detrimental effects of NMF on proprioceptive feedback. This interference likely results in altered proprioceptive input to the cerebellum, adversely affecting the sensory prediction accuracy crucial for implicit learning. Additionally, the compromised performance observed in the later stages of adaptation could also be linked to the cerebellum's role in perceiving fatigue (30). Such mechanisms are suggested to hinder motor learning, suggesting that the observed performance variations under fatigue conditions might arise from an increased cerebellar involvement in both perceiving fatigue and facilitating motor adaptation.

Our findings diverge to some extent from the results of Takahashi et al. (40), who reported no impact of NMF on motor adaptation in reaching tasks. This discrepancy may stem from differences in experimental design. Specifically, Takahashi et al.'s participants initially adapted to the reaching task without fatigue, potentially achieving performance stabilization before encountering NMF. Additionally, their adaptation phase was limited to 20 trials, possibly too short for highlighting long-term differences. Another possible explanation might arise from the different fatiguing protocols between the study by Takahashi and the present one. In their study they fatigued participants' effector muscles (i.e. muscles in the upper limb) during resisted reaching movements, which possibly allowed the CNS to process and integrate proprioceptive signals coming from the fatigued muscles (i.e. group III and IV afferences (81, 82)) prior to the following execution of the retention tests.

Fatigue-Induced Changes In EMG Activation and Co-Activation Patterns

EMG analysis revealed divergent activation patterns in the musculature of the upper and lower limbs between subjects in the Fatigue and No-Fatigue groups throughout the experimental stages. Specifically, individuals in the Fatigue group exhibited higher levels of muscle activity in the upper extremity, alongside lower levels of activity in the leg muscles, as depicted in **Figure 4**. Notably, differences in EMG activation were primarily observed in the left-side postural muscles. This observation aligns with the mechanism where, during a directional reaching task, postural muscles on the body's left side are activated earlier than the onset of the reaching action (83). This preemptive activation serves to stabilize posture in anticipation of a volitional movement towards the right. Our findings provide support for studies that have shown feedforward modulation of lower limb muscle activity in relation to the direction of movement (83–85).

The observed decrease in lower-limb muscle activation, particularly during the anticipatory phase, in the Fatigue group implies that fatigue affects the pre-programming of movements involving postural muscles. Leonard and colleagues suggested that anticipatory activity in the left-side postural muscles is evidence of CNS mechanisms at play (83). The diminished or absent anticipatory activity in both the fatigued muscle (e.g., tibialis anterior) and the non-fatigued muscle (e.g., rectus femoris) in the Fatigue group indicates that the fatiguing exercise exerted a widespread impact, affecting motor planning at the central level. This finding aligns with prior studies on the effects of localized fatigue on motor control (17, 23) and, to our understanding, marks a clear demonstration of such neural drive reorganization during motor adaptation. Conversely, the Fatigue group also exhibited increased activation of the anterior deltoid (AD) muscle, alongside more frequent adjustments in hand movement trajectory—as evidenced by higher hand path variability (HPV) values (**Figure 3**)—suggesting a greater reliance on visual input for correcting movement trajectories. This may be an attempt to offset the unreliable proprioceptive feedback from fatigued muscles (14, 82, 86). Additionally, the elevated AD muscle activity during the anticipatory phase suggests that participants pre-activated this muscle to enhance its response to force field disturbances, thereby increasing the muscle's "apparent stiffness" (87).

The observed patterns of muscle co-activation among agonist-antagonist pairs at the joint level were consistent with the results obtained from individual EMG assessments. In the No-Fatigue group, there was an increase in co-activation of left-side postural muscles, while in the Fatigue group, an increase in co-activation was noted among upper-limb muscles. These contrasting trends indicate that the CNS implemented different strategies throughout the adaptation process to maintain postural stability in the face of localized neuromuscular fatigue (NMF).

In managing standing posture, two strategies may be employed: 1) enhancing joint stiffness through increased muscle co-activation to stabilize the joints (87) or 2) decreasing muscle co-activation, thereby tolerating greater postural variability but allowing for focused EMG activation to preserve postural stability (88). Our findings indicate a strategy divergence between two groups, with the Fatigue group preferring the second approach. This is consistent with recent findings in scenarios involving pendulum-like perturbations and increased postural threat (60). Cesari et al. (60) proposed that reducing muscle co-contraction is a more prudent approach under challenging conditions, such as heightened fall risk. Regarding localized neuromuscular fatigue (NMF), two mechanisms—impaired proprioception and suboptimal neuromuscular response, either separately or in combination—may account for these varying strategies.

First, NMF is known to result in impaired proprioception due to neuromechanical and chemical alterations both at the level of the muscle fibers and in terms of antidromic afferent signaling to the CNS (82, 89). This distorted feedback likely disrupts

sensorimotor integration, prompting a conservative reduction in agonist-antagonist co-activation and compelling the CNS to adopt alternative strategies, such as activating other muscle groups. This adaptation mirrors the modulation in pre-planned and reactive muscle activation, as well as co-contraction observed in experiments involving mechanical disruption of muscle proprioception through tendon vibration (57, 86). Secondly, the fatigued muscle's reduced capacity to respond effectively to postural perturbations might be another factor. Early studies reported delayed muscle response times after NMF (90, 91). A more recent investigation found a decrease in intra-muscle force-stabilizing synergies within tibialis anterior motor units during a force-tracking task post-NMF, indicating a potential impairment in spinal reflex loops due to fatigue (43).

Collectively, the alterations in muscle responsiveness induced by localized NMF may compromise a muscle's efficiency in counteracting disturbances to postural stability caused by external force fields. We propose that both identified mechanisms—impaired proprioception and a diminished neuromuscular response—could elucidate the observed divergence in muscle activation patterns. These findings suggest that the CNS is prompted to adopt alternative strategies to manage postural perturbations in the context of fatigue.

In conclusion, our findings indicate that localized neuromuscular fatigue (NMF) adversely affects the adaptation of reaching movements in response to force field perturbations. This impairment does not stem from a reduction in postural stability, which remains intact following NMF, but is likely due to compromised sensorimotor integration, particularly in processing proprioceptive and sensory feedback during fatigue. Notably, the cerebellum's critical role in motor adaptation may underlie these observed discrepancies. Our study also reveals variations in the activation of both fatigued and non-fatigued muscles, as well as in the strategies for correcting movements, indicating that the physiological disruptions caused by NMF during force field perturbations could prompt the selection of alternative motor adaptation strategies. Future research should investigate whether these adaptations are temporary, resolving with recovery, or if they have lasting impacts on the retention of these newly adopted strategies.

The implications of our findings extend to scenarios where NMF may occur in the context of learning motor skills, such as in sports and recreational activities, or in rehabilitation settings where relearning a motor task or skill is necessary under conditions more susceptible to NMF, like in cases of cerebral palsy, multiple sclerosis, or stroke.

SUPPLEMENTAL MATERIAL

Available at OSF: https://osf.io/hgpu9/ (DOI 10.17605/OSF.IO/HGPU9)

S1 – Upper limb & right-side muscles EMGs (Text, Figures & Tables)

S2 – Dorsal EMGs (Text, Figures & Tables)

S3 – Left EMGs washout (Figure)

S4 – Right C-index (Figures & Tables)

S5 – Left C-index washout (Figure)

S6 – CoP variables washout (Figure)

References

1. **Bigland-Ritchie B**, **Furbush F**, **Woods JJ**. Fatigue of intermittent submaximal voluntary contractions: central and peripheral factors. *J Appl Physiol* 61: 421–429, 1986. doi: 10.1152/jappl.1986.61.2.421.

2. **Gandevia SC**. Spinal and supraspinal factors in human muscle fatigue. *Physiol Rev* 81: 1725–1789, 2001. doi: 10.1152/physrev.2001.81.4.1725.

3. **Enoka RM**, **Duchateau J**. Muscle fatigue: what, why and how it influences muscle function: Muscle fatigue. *J Physiol* 586: 11–23, 2008. doi: 10.1113/jphysiol.2007.139477.

4. **Strang AJ**, **Berg WP**. Fatigue-induced adaptive changes of anticipatory postural adjustments. *Exp Brain Res* 178: 49–61, 2007. doi: 10.1007/s00221-006-0710-5.

5. **Gates DH**, **Dingwell JB**. The effects of neuromuscular fatigue on task performance during repetitive goal-directed movements. *Exp Brain Res* 187: 573–585, 2008.

6. **Kanekar N**, **Santos MJ**, **Aruin AS**. Anticipatory postural control following fatigue of postural and focal muscles. *Clin Neurophysiol* 119: 2304–2313, 2008. doi: 10.1016/j.clinph.2008.06.015.

7. **Strang AJ**, **Berg WP**, **Hieronymus M**. Fatigue-induced early onset of anticipatory postural adjustments in non-fatigued muscles: support for a centrally mediated adaptation. *Exp Brain Res* 197: 245–254, 2009. doi: 10.1007/s00221-009-1908-0.

8. **Forestier N**, **Nougier V**. The effects of muscular fatigue on the coordination of a multijoint movement in human. *Neurosci Lett* 252: 187–190, 1998. doi: 10.1016/S0304-3940(98)00584-9.

9. **Coventry E**, **O'Connor KM**, **Hart BA**, **Earl JE**, **Ebersole KT**. The effect of lower extremity fatigue on shock attenuation during single-leg landing. *Clin Biomech* 21: 1090–1097, 2006. doi: 10.1016/j.clinbiomech.2006.07.004.

10. **Singh T**, **SKM V**, **Zatsiorsky VM**, **Latash ML**. Fatigue and motor redundancy: adaptive increase in finger force variance in multi-finger tasks. *J Neurophysiol* 103: 2990–3000, 2010.

11. **Singh T**, **Zatsiorsky VM**, **Latash ML**. Contrasting effects of fatigue on multi-finger coordination in young and older adults. *J Appl Physiol* 115: 456–467, 2013.

12. **Nardone A**, **Tarantola J**, **Giordano A**, **Schieppati M**. Fatigue effects on body balance. *Electroencephalogr Clin Neurophysiol* 105: 309–320, 1997. doi: 10.1016/s0924-980x(97)00040-4.

13. **Vuillerme N**, **Boisgontier M**. Muscle fatigue degrades force sense at the ankle joint. *Gait Posture* 28: 521–524, 2008. doi: 10.1016/j.gaitpost.2008.03.005.

14. **Albanese GA**, **Falzarano V**, **Holmes MWR**, **Morasso P**, **Zenzeri J**. A Dynamic Submaximal Fatigue Protocol Alters Wrist Biomechanical Properties and Proprioception [Online]. *Front Hum Neurosci* 16, 2022. https://www.frontiersin.org/articles/10.3389/fnhum.2022.887270 [12 Jul. 2022].

15. **Vafadar AK**, **Côté J**, **Archambault PS**. The effect of muscle fatigue on position sense in an upper limb multi-joint task. *Motor Control* 16: 265–283, 2012.

16. **Grose G**, **Manzone DM**, **Eschelmuller G**, **Peters RM**, **Carpenter MG**, **Inglis JT**, **Chua R**. The effects of eccentric exercise-induced fatigue on position sense during goal-directed movement. *J Appl Physiol* 132: 1005–1019, 2022. doi: 10.1152/japplphysiol.00177.2021.

17. **Singh T**, **Latash ML**. Effects of muscle fatigue on multi-muscle synergies. *Exp Brain Res* 214: 335–350, 2011. doi: 10.1007/s00221-011-2831-8.

18. **Segers V**, **Lenoir M**, **Aerts P**, **De Clercq D**. Influence of M. tibialis anterior fatigue on the walk-to-run and run-to-walk transition in non-steady state locomotion. *Gait Posture* 25: 639–647, 2007. doi: 10.1016/j.gaitpost.2006.07.008.

19. **Parijat P**, **Lockhart TE**. Effects of quadriceps fatigue on the biomechanics of gait and slip propensity. *Gait Posture* 28: 568–573, 2008. doi: 10.1016/j.gaitpost.2008.04.001.

20. **Qu X**, **Yeo JC**. Effects of load carriage and fatigue on gait characteristics. *J Biomech* 44: 1259–1263, 2011. doi: 10.1016/j.jbiomech.2011.02.016.

21. **Barbieri FA**, **dos Santos PCR**, **Vitório R**, **van Dieën JH**, **Gobbi LTB**. Effect of muscle fatigue and physical activity level in motor control of the gait of young adults. *Gait Posture* 38: 702–707, 2013. doi: 10.1016/j.gaitpost.2013.03.006.

22. **Gribble PA**, **Hertel J**. Effect of lower-extremity muscle fatigue on postural control1. *Arch Phys Med Rehabil* 85: 589–592, 2004. doi: 10.1016/j.apmr.2003.06.031.

23. **Lyu H**, **Fan Y**, **Hao Z**, **Wang J**. Effect of local and general fatiguing exercises on disturbed and static postural control. *J Electromyogr Kinesiol* 56: 102487, 2021. doi: 10.1016/j.jelekin.2020.102487.

24. **Lyu H**, **Fan Y**, **Hua A**, **Cao X**, **Gao Y**, **Wang J**. Effects of unilateral and bilateral lower extremity fatiguing exercises on postural control during quiet stance and self-initiated perturbation. *Hum Mov Sci* 81: 102911, 2022. doi: 10.1016/j.humov.2021.102911.

25. **Davidson BS**, **Madigan ML**, **Nussbaum MA**, **Wojcik LA**. Effects of localized muscle fatigue on recovery from a postural perturbation without stepping. *Gait Posture* 29: 552–557, 2009. doi: 10.1016/j.gaitpost.2008.12.011.

26. **Marcolin G**, **Cogliati M**, **Cudicio A**, **Negro F**, **Tonin R**, **Orizio C**, **Paoli A**. Neuromuscular Fatigue Affects Calf Muscle Activation Strategies, but Not Dynamic Postural Balance Control in Healthy Young Adults [Online]. *Front Physiol* 13, 2022. https://www.frontiersin.org/articles/10.3389/fphys.2022.799565 [27 Nov. 2023].

27. **Paillard T**, **Chaubet V**, **Maitre J**, **Dumitrescu M**, **Borel L**. Disturbance of contralateral unipedal postural control after stimulated and voluntary contractions of the ipsilateral limb. *Neurosci Res* 68: 301–306, 2010. doi: 10.1016/j.neures.2010.08.004.

28. **Singh T**, **Zatsiorsky VM**, **Latash ML**. Effects of fatigue on synergies in a hierarchical system. *Hum Mov Sci* 31: 1379–1398, 2012.

29. **Halperin I**, **Chapman DW**, **Behm DG**. Non-local muscle fatigue: effects and possible mechanisms. .

30. **Casamento-Moran A**, **Mooney RA**, **Chib VS**, **Celnik PA**. Cerebellar excitability regulates physical fatigue perception. *J Neurosci* 43: 3094–3106, 2023.

31. **Debaere F**, **Wenderoth N**, **Sunaert S**, **Van Hecke P**, **Swinnen SP**. Cerebellar and premotor function in bimanual coordination: parametric neural responses to spatiotemporal complexity and cycling frequency. *Neuroimage* 21: 1416–1427, 2004.

32. **Soteropoulos DS**, **Baker SN**. Bilateral representation in the deep cerebellar nuclei. *J Physiol* 586: 1117–1136, 2008.

33. **Debaere F**, **Swinnen SP**, **Béatse E**, **Sunaert S**, **Van Hecke P**, **Duysens J**. Brain areas involved in interlimb coordination: A distributed network. *NeuroImage* 14: 947–958, 2001. doi: 10.1006/nimg.2001.0892.

34. **Maschke M**, **Gomez CM**, **Ebner TJ**, **Konczak J**. Hereditary cerebellar ataxia progressively impairs force adaptation during goal-directed arm movements. *J Neurophysiol* 91: 230–238, 2004.

35. **Smith MA**, **Shadmehr R**. Intact ability to learn internal models of arm dynamics in Huntington's disease but not cerebellar degeneration. *J Neurophysiol* 93: 2809–2821, 2005.

36. **Criscimagna-Hemminger SE**, **Bastian AJ**, **Shadmehr R**. Size of error affects cerebellar contributions to motor learning. *J Neurophysiol* 103: 2275–2284, 2010.

37. **Donchin O**, **Rabe K**, **Diedrichsen J**, **Lally N**, **Schoch B**, **Gizewski ER**, **Timmann D**. Cerebellar regions involved in adaptation to force field and visuomotor perturbation. *J Neurophysiol* 107: 134–147, 2012.

38. **Statton MA**, **Vazquez A**, **Morton SM**, **Vasudevan EVL**, **Bastian AJ**. Making sense of cerebellar contributions to perceptual and motor adaptation. *The Cerebellum* 17: 111–121, 2018. doi: 10.1007/s12311-017-0879-0.

39. **Shadmehr R**, **Mussa-Ivaldi FA**. Adaptive representation of dynamics during learning of a motor task. *J Neurosci* 14: 3208–3224, 1994.

40. **Takahashi CD**, **Nemet D**, **Rose-Gottron CM**, **Larson JK**, **Cooper DM**, **Reinkensmeyer DJ**. Effect of muscle fatigue on internal model formation and retention during reaching with the arm. *J Appl Physiol* 100: 695–706, 2006. doi: 10.1152/japplphysiol.00140.2005.

41. **Ahmed AA**, **Wolpert DM**. Transfer of dynamic learning across postures. *J Neurophysiol* 102: 2816–2824, 2009. doi: 10.1152/jn.00532.2009.

42. **Hermens HJ**, **Freriks B**, **Disselhorst-Klug C**, **Rau G**. Development of recommendations for SEMG sensors and sensor placement procedures. *J Electromyogr Kinesiol* 10: 361–374, 2000.

43. **Ricotta JM**, **De SD**, **Nardon M**, **Benamati A**, **Latash ML**. Effects of fatigue on intramuscle force-stabilizing synergies. *J Appl Physiol Bethesda Md 1985* 135: 1023–1035, 2023. doi: 10.1152/japplphysiol.00419.2023.

44. **Carroll TJ**, **Taylor JL**, **Gandevia SC**. Recovery of central and peripheral neuromuscular fatigue after exercise. *J Appl Physiol* 122: 1068–1076, 2017.

45. **Enoka RM**, **Stuart DG**. Neurobiology of muscle fatigue. *J Appl Physiol* 72: 1631–1648, 1992.

46. **Pienciak-Siewert A**, **Horan DP**, **Ahmed AA**. Trial-to-trial adaptation in control of arm reaching and standing posture. *J Neurophysiol* 116: 2936–2949, 2016. doi: 10.1152/jn.00537.2016.

47. **Pienciak-Siewert A**, **Horan DP**, **Ahmed AA**. Role of muscle coactivation in adaptation of standing posture during arm reaching. *J Neurophysiol* 123: 529–547, 2020. doi: 10.1152/jn.00939.2017.

48. **Sinha O**, **Madarshahian S**, **Gómez-Granados A**, **Paine ML**, **Kurtzer I**, **Singh T**. Smooth pursuit eye movements contribute to anticipatory force control during mechanical stopping of moving objects. *J Neurophysiol* 129: 1293–1309, 2023. doi: 10.1152/jn.00075.2023.

49. **Malone LA**, **Vasudevan EVL**, **Bastian AJ**. Motor Adaptation Training for Faster Relearning. *J Neurosci* 31: 15136–15143, 2011. doi: 10.1523/JNEUROSCI.1367-11.2011.

50. **Winter DA**. *Biomechanics and motor control of human movement*. 4th ed. Hoboken, N.J: Wiley, 2009.

51. **Horak FB**, **Nashner LM**. Central programming of postural movements: adaptation to altered support-surface configurations. *J Neurophysiol* 55: 1369–1381, 1986. doi: 10.1152/jn.1986.55.6.1369.

52. **Krishnan V**, **Kanekar N**, **Aruin AS**. Anticipatory postural adjustments in individuals with multiple sclerosis. *Neurosci Lett* 506: 256–260, 2012. doi: 10.1016/j.neulet.2011.11.018.

53. **Scott SH**, **Cluff T**, **Lowrey CR**, **Takei T**. Feedback control during voluntary motor actions. *Curr Opin Neurobiol* 33: 85–94, 2015. doi: 10.1016/j.conb.2015.03.006.

54. **Nardone A**, **Schieppati M**. Postural adjustments associated with voluntary contraction of leg muscles in standing man. *Exp Brain Res* 69: 469–480, 1988. doi: 10.1007/BF00247301.

55. **Feldman AG**. Once more on the equilibrium-point hypothesis (lambda model) for motor control. *J Mot Behav* 18: 17–54, 1986. doi: 10.1080/00222895.1986.10735369.

56. **Slijper H**, **Latash M**. The effects of instability and additional hand support on anticipatory postural adjustments in leg, trunk, and arm muscles during standing. *Exp Brain Res* 135: 81–93, 2000. doi: 10.1007/s002210000492.

57. **Slijper H**, **Latash ML**. The effects of muscle vibration on anticipatory postural adjustments. *Brain Res* 1015: 57–72, 2004. doi: 10.1016/j.brainres.2004.04.054.

58. **Piscitelli D**, **Falaki A**, **Solnik S**, **Latash ML**. Anticipatory postural adjustments and anticipatory synergy adjustments: Preparing to a postural perturbation with predictable and unpredictable direction. *Exp Brain Res* 235: 713–730, 2017. doi: 10.1007/s00221-016-4835-x.

59. **Bertucco M**, **Nardello F**, **Magris R**, **Cesari P**, **Latash ML**. Postural Adjustments during Interactions with an Active Partner. *Neuroscience* 463: 14–29, 2021. doi: 10.1016/j.neuroscience.2021.03.020.

60. **Cesari P**, **Piscitelli F**, **Pascucci F**, **Bertucco M**. Postural threat influences the coupling between anticipatory and compensatory postural adjustments in response to an external perturbation. .

61. **Paillard T**. Effects of general and local fatigue on postural control: A review. *Neurosci Biobehav Rev* 36: 162–176, 2012. doi: 10.1016/j.neubiorev.2011.05.009.

62. **Zemková E**, **Hamar D**. Physiological mechanisms of post-exercise balance impairment. *Sports Med Auckl NZ* 44: 437–448, 2014. doi: 10.1007/s40279-013-0129-7.

63. **Donath L**, **Kurz E**, **Roth R**, **Zahner L**, **Faude O**. Different ankle muscle coordination patterns and co-activation during quiet stance between young adults and seniors do not change after a bout of high intensity training. *BMC Geriatr* 15: 19, 2015. doi: 10.1186/s12877-015-0017-0.

64. **Barbieri FA**, **Beretta SS**, **Pereira VAI**, **Simieli L**, **Orcioli-Silva D**, **dos Santos PCR**, **van Dieën JH**, **Gobbi LTB**. Recovery of gait after quadriceps muscle fatigue. *Gait Posture* 43: 270–274, 2016. doi: 10.1016/j.gaitpost.2015.10.015.

65. **Jo D**, **Bilodeau M**. Sex differences concerning the effects of ankle muscle fatigue on static postural control and spinal proprioceptive input at the ankle. *Front Hum Neurosci* 17: 1015597, 2023. doi: 10.3389/fnhum.2023.1015597.

66. **Taylor JL**, **Butler JE**, **Gandevia SC**. Changes in muscle afferents, motoneurons and motor drive during muscle fatigue. *Eur J Appl Physiol* 83: 106–115, 2000. doi: 10.1007/s004210000269.

67. **Carroll TJ**, **Taylor JL**, **Gandevia SC**. Recovery of central and peripheral neuromuscular fatigue after exercise. *J Appl Physiol* 122: 1068–1076, 2017. doi: 10.1152/japplphysiol.00775.2016.

68. **Smith MA**, **Ghazizadeh A**, **Shadmehr R**. Interacting Adaptive Processes with Different Timescales Underlie Short-Term Motor Learning. *PLOS Biol* 4: e179, 2006. doi: 10.1371/journal.pbio.0040179.

69. **McDougle SD**, **Bond KM**, **Taylor JA**. Explicit and Implicit Processes Constitute the Fast and Slow Processes of Sensorimotor Learning. *J Neurosci Off J Soc Neurosci* 35: 9568–9579, 2015. doi: 10.1523/JNEUROSCI.5061-14.2015.

70. **Taylor JA**, **Krakauer JW**, **Ivry RB**. Explicit and Implicit Contributions to Learning in a Sensorimotor Adaptation Task. *J Neurosci* 34: 3023–3032, 2014. doi: 10.1523/JNEUROSCI.3619-13.2014.

71. **Butcher PA**, **Ivry RB**, **Kuo S-H**, **Rydz D**, **Krakauer JW**, **Taylor JA**. The cerebellum does more than sensory prediction error-based learning in sensorimotor adaptation tasks. *J Neurophysiol* 118: 1622–1636, 2017. doi: 10.1152/jn.00451.2017.

72. **Haar S**, **Donchin O**. A Revised Computational Neuroanatomy for Motor Control. *J Cogn Neurosci* 32: 1823–1836, 2020. doi: 10.1162/jocn_a_01602.

73. **Izawa J**, **Criscimagna-Hemminger SE**, **Shadmehr R**. Cerebellar Contributions to Reach Adaptation and Learning Sensory Consequences of Action. *J Neurosci* 32: 4230–4239, 2012. doi: 10.1523/JNEUROSCI.6353-11.2012.

74. **Schlerf JE**, **Xu J**, **Klemfuss NM**, **Griffiths TL**, **Ivry RB**. Individuals with cerebellar degeneration show similar adaptation deficits with large and small visuomotor errors. *J Neurophysiol* 109: 1164–1173, 2013. doi: 10.1152/jn.00654.2011.

75. **Tseng Y-W**, **Diedrichsen J**, **Krakauer JW**, **Shadmehr R**, **Bastian AJ**. Sensory prediction errors drive cerebellum-dependent adaptation of reaching. *J Neurophysiol* 98: 54–62, 2007. doi: 10.1152/jn.00266.2007.

76. **Taylor JA**, **Ivry RB**. Cerebellar and prefrontal cortex contributions to adaptation, strategies, and reinforcement learning. *Prog Brain Res* 210: 217–253, 2014. doi: 10.1016/B978-0-444-63356-9.00009-1.

77. **Weeks HM**, **Therrien AS**, **Bastian AJ**. The cerebellum contributes to proprioception during motion. *J Neurophysiol* 118: 693–702, 2017. doi: 10.1152/jn.00417.2016.

78. **Tsay JS**, **Kim H**, **Haith AM**, **Ivry RB**. Understanding implicit sensorimotor adaptation as a process of proprioceptive re-alignment. *eLife* 11: e76639, 2022. doi: 10.7554/eLife.76639.

79. **Proske U**. Exercise, fatigue and proprioception: a retrospective. *Exp Brain Res* 237: 2447–2459, 2019. doi: 10.1007/s00221-019-05634-8.

80. **Mangalam M**, **Cuadra C**, **Singh T**. Sensory redundancy and perceptual invariance in force production and object manipulation. *Curr Opin Physiol* 19: 148–155, 2021. doi: 10.1016/j.cophys.2020.11.002.

81. **Amann M**, **Blain GM**, **Proctor LT**, **Sebranek JJ**, **Pegelow DF**, **Dempsey JA**. Group III and IV muscle afferents contribute to ventilatory and cardiovascular response to rhythmic exercise in humans. *J Appl Physiol* 109: 966–976, 2010. doi: 10.1152/japplphysiol.00462.2010.

82. **Sidhu SK**, **Weavil JC**, **Mangum TS**, **Jessop JE**, **Richardson RS**, **Morgan DE**, **Amann M**. Group III/IV locomotor muscle afferents alter motor cortical and corticospinal excitability and promote central fatigue during cycling exercise. *Clin Neurophysiol* 128: 44–55, 1AD. doi: 10.1016/j.clinph.2016.10.008.

83. **Leonard JA**, **Gritsenko V**, **Ouckama R**, **Stapley PJ**. Postural adjustments for online corrections of arm movements in standing humans. *J Neurophysiol* 105: 2375–2388, 2011. doi: 10.1152/jn.00944.2010.

84. **Leonard JA**, **Brown RH**, **Stapley PJ**. Reaching to Multiple Targets When Standing: The Spatial Organization of Feedforward Postural Adjustments. *J Neurophysiol* 101: 2120–2133, 2009. doi: 10.1152/jn.91135.2008.

85. **Lowrey CR**, **Nashed JY**, **Scott SH**. Rapid and flexible whole body postural responses are evoked from perturbations to the upper limb during goal-directed reaching. *J Neurophysiol* 117: 1070–1083, 2017. doi: 10.1152/jn.01004.2015.

86. **Mohapatra S**, **Krishnan V**, **Aruin AS**. Postural control in response to an external perturbation: effect of altered proprioceptive information. *Exp Brain Res* 217: 197–208, 2012. doi: 10.1007/s00221-011-2986-3.

87. **Latash ML**, **Zatsiorsky VM**. Joint stiffness: Myth or reality? *Hum Mov Sci* 12: 653–692, 1993. doi: 10.1016/0167-9457(93)90010-M.

88. **Latash ML**. Muscle coactivation: definitions, mechanisms, and functions. *J Neurophysiol* 120: 88–104, 2018. doi: 10.1152/jn.00084.2018.

89. **Amann M**, **Venturelli M**, **Ives SJ**, **McDaniel J**, **Layec G**, **Rossman MJ**, **Richardson RS**. Peripheral fatigue limits endurance exercise via a sensory feedback-mediated reduction in spinal motoneuronal output. *J Appl Physiol Bethesda Md 1985* 115: 355–364, 2013. doi: 10.1152/japplphysiol.00049.2013.

90. **Balestra C**, **Duchateau J**, **Hainaut K**. Effects of fatigue on the stretch reflex in a human muscle. *Electroencephalogr Clin Neurophysiol Potentials Sect* 85: 46–52, 1992. doi: 10.1016/0168-5597(92)90101-G.

91. **Duchateau J**, **Hainaut K**. Behaviour of short and long latency reflexes in fatigued human muscles. *J Physiol* 471: 787–799, 1993. doi: 10.1113/jphysiol.1993.sp019928.

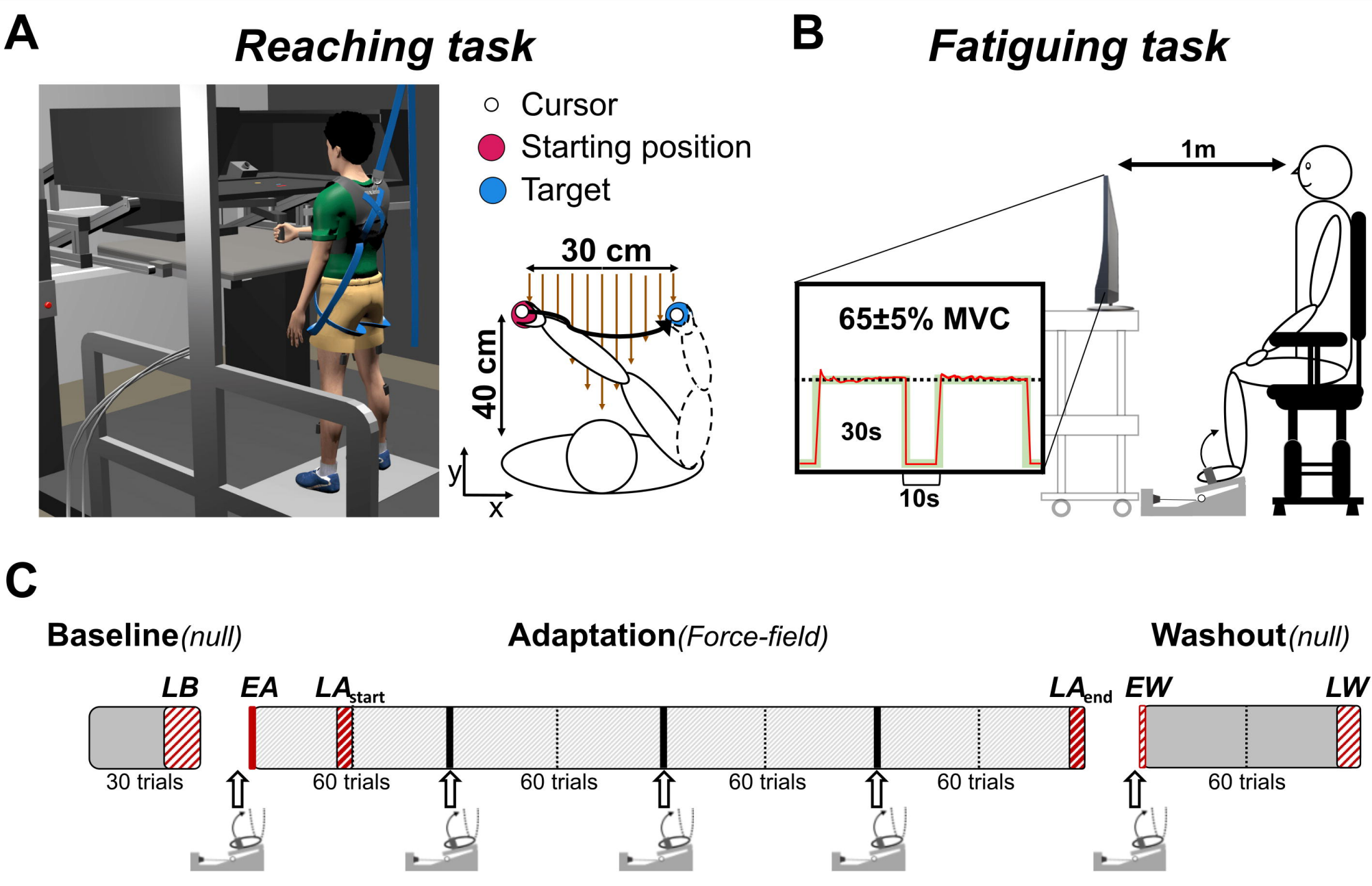
A
Reaching task
Cursor
Starting position
Target
30 cm
40 cm
y
x
B
Fatiguing task
1m
65±5% MVC
30s
10s
C
Baseline(null)
Adaptation(Force-field)
Washout(null)
LB
EA
LAstart
LAend
EW
LW
30 trials
60 trials
60 trials
60 trials
60 trials
60 trials

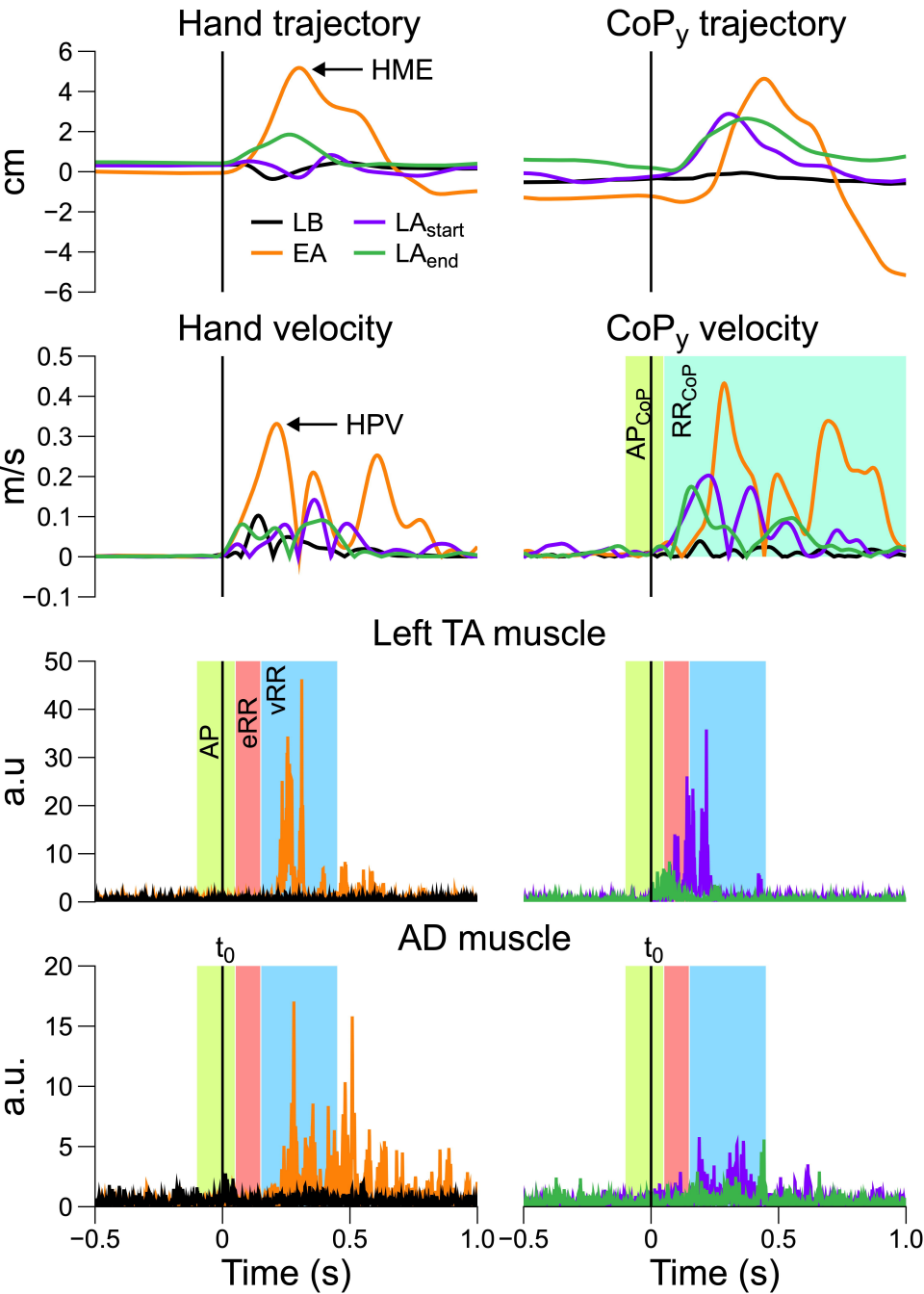
Hand trajectory
CoPy trajectory
HME
cm
6
4
2
0
−2
−4
−6
LB
EA
LAstart
LAend
Hand velocity
CoPy velocity
HPV
m/s
0.5
0.4
0.3
0.2
0.1
0
−0.1
APCoP
RRCoP
Left TA muscle
AP
eRR
vRR
a.u
50
40
30
20
10
0
AD muscle
t0
t0
a.u.
20
15
10
5
0
−0.5
0
0.5
1.0
Time (s)
Time (s)

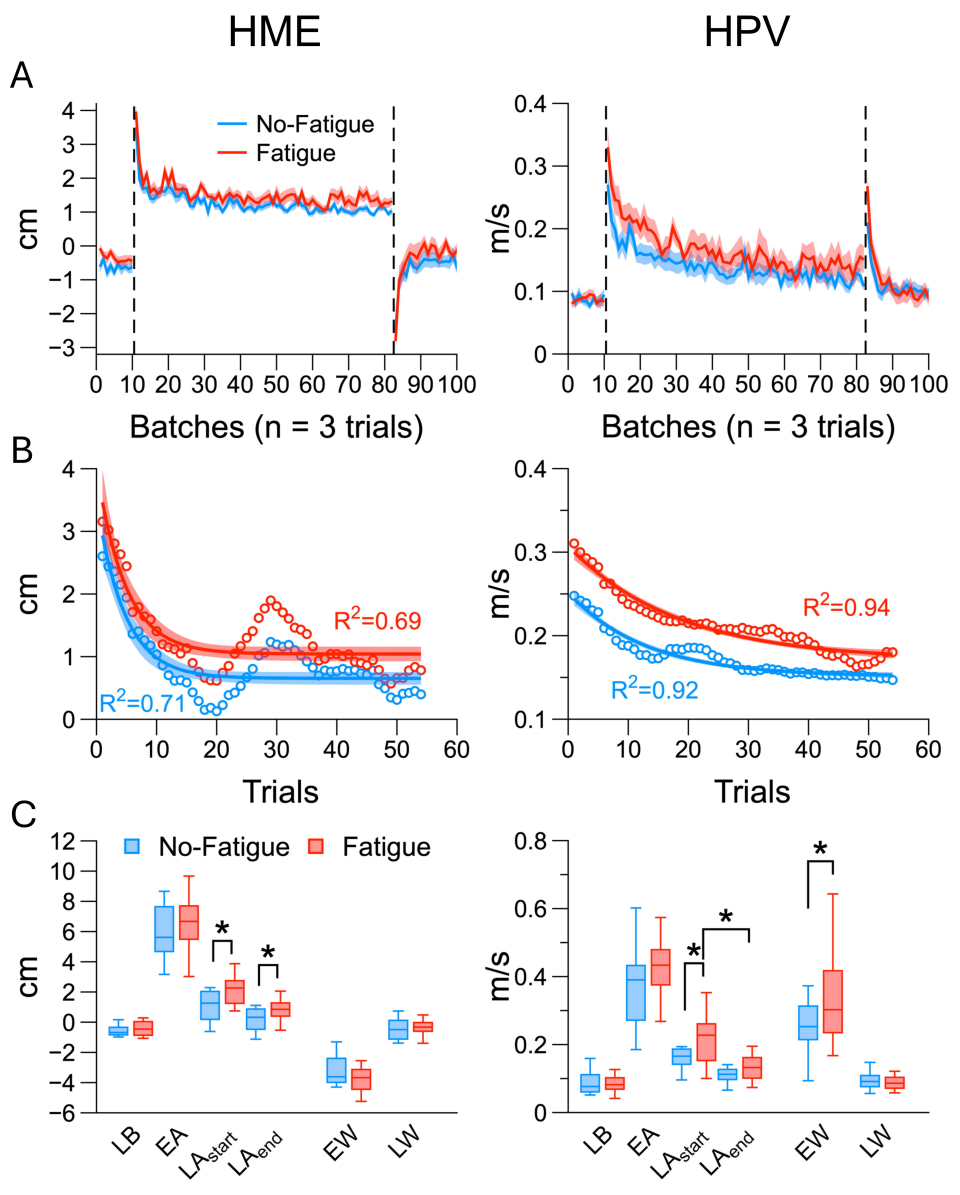
HME
HPV
A
No-Fatigue
Fatigue
cm
m/s
Batches (n = 3 trials)
B
R2=0.69
R2=0.71
R2=0.94
R2=0.92
Trials
C
LB
EA
LAstart
LAend
EW
LW

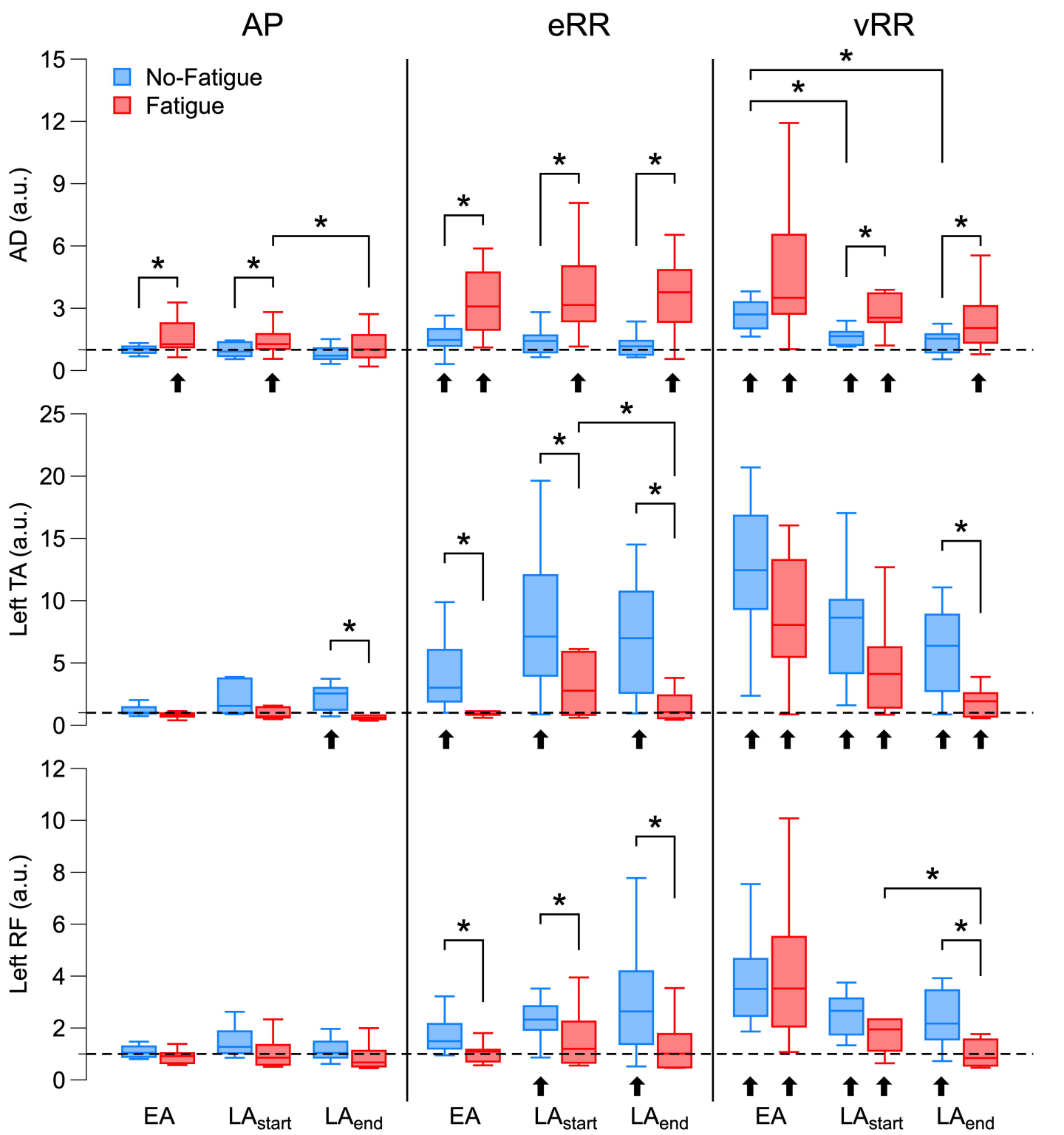
AP
eRR
vRR
No-Fatigue
Fatigue
AD (a.u.)
Left TA (a.u.)
Left RF (a.u.)
EA
LAstart
LAend

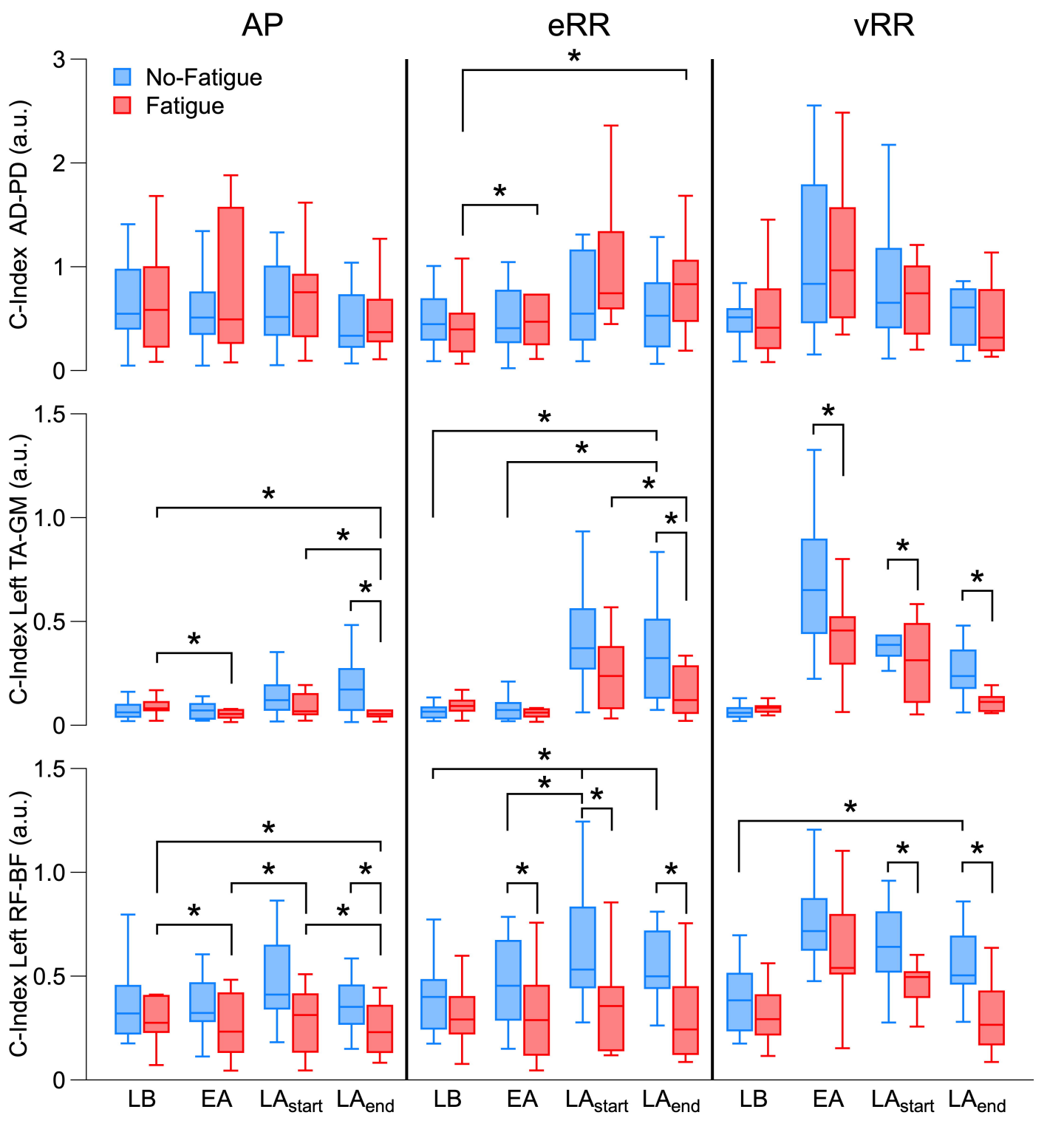
AP
eRR
vRR
No-Fatigue
Fatigue
C-Index AD-PD (a.u.)
C-Index Left TA-GM (a.u.)
C-Index Left RF-BF (a.u.)
LB
EA
LAstart
LAend

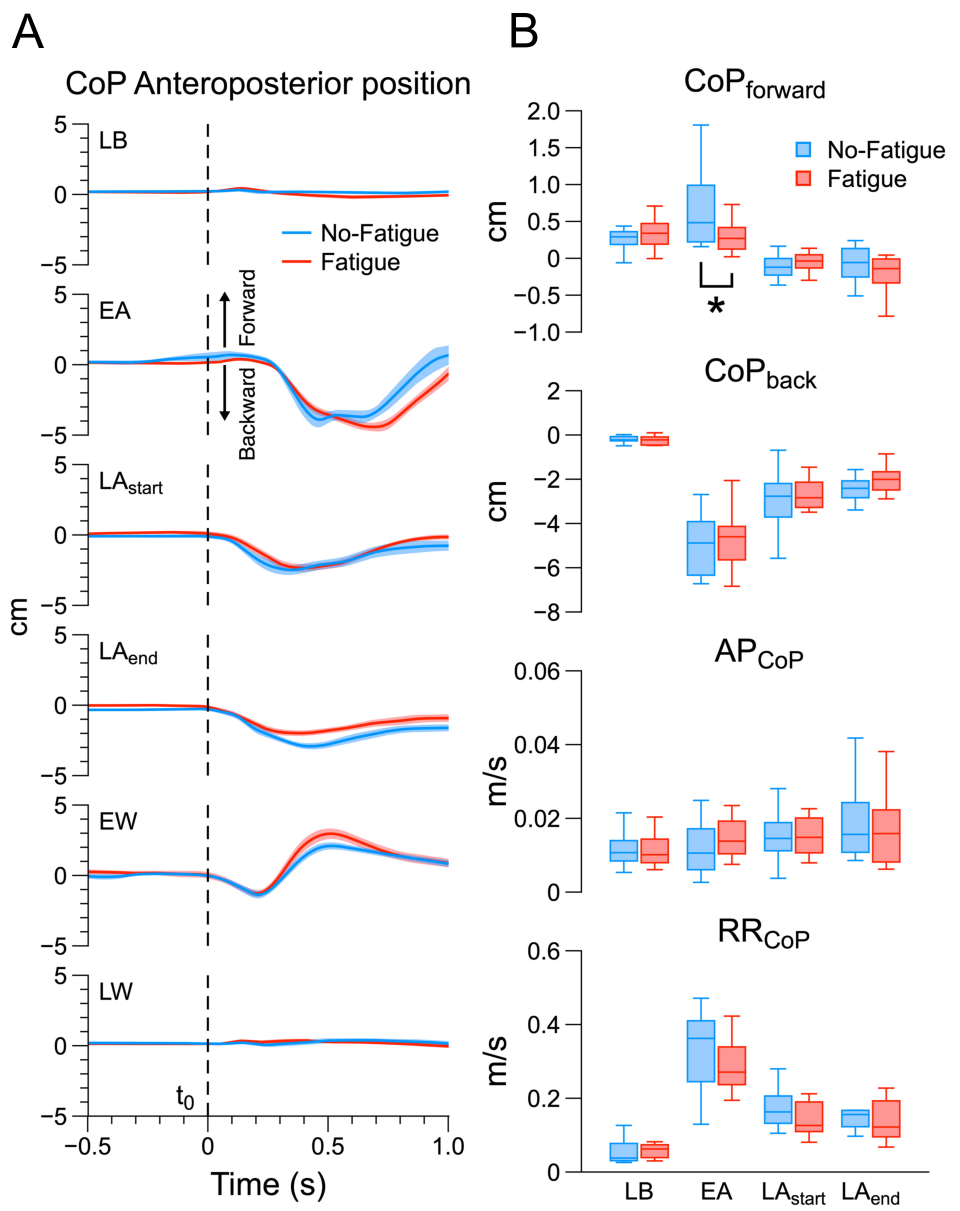
A
CoP Anteroposterior position
LB
EA
LAstart
LAend
EW
LW
No-Fatigue
Fatigue
Forward
Backward
cm
t0
Time (s)
B
CoPforward
CoPback
APCoP
RRCoP
No-Fatigue
Fatigue
cm
m/s
*
LB
EA
LAstart
LAend